University of Alaska

Coastal Marine Institute

Proceedings of a Workshop

on

Small-Scale Sea-Ice and Ocean Modeling (SIOM) in the Nearshore Beaufort and Chukchi Seas

Jia Wang, Principal Investigator
University of Alaska Fairbanks

Final Report

July 2003

OCS Study MMS 2003-043

Final Report

Proceedings of a Workshop

on

Small-Scale Sea-Ice and Ocean Modeling (SIOM) in the Nearshore Beaufort and Chukchi Seas

by

Jia Wang
Principal Investigator

Frontier Research System for Global Change
International Arctic Research Center
University of Alaska Fairbanks
Fairbanks, AK 99775-7335

E-mail: jwang@iarc.uaf.edu

July 2003

Contact information

e-mail: cmi@sfos.uaf.edu
phone: 907.474.7707
   fax: 907.474.7204
postal: Coastal Marine Institute
        School of Fisheries and Ocean Sciences
        University of Alaska Fairbanks
        Fairbanks, AK 99775-7220

Table of Contents

List of Figures

Abstract

A workshop on small-scale *Sea-Ice* and *Ocean Modeling* (SIOM) for the nearshore Beaufort and Chukchi seas was held at the International Arctic Research Center (IARC), University of Alaska Fairbanks (UAF) 7–9 August 2002 (http://www.frontier.iarc.uaf.edu:8080/SIOM-Workshop-02). This workshop was jointly sponsored by the Minerals Management Service (MMS)/U.S. Department of the Interior, Coastal Marine Institute/UAF, and the IARC-Frontier Research System for Global Change (IARC-Frontier).

One of the objectives of this workshop was to bring modelers and observers together to discuss strategies for state-of-the-art ice–ocean modeling. The workshop highlighted approaches to small-scale and regional ice–ocean modeling that could be applied to the nearshore Beaufort and Chukchi seas, including seasonal landfast ice, based on satellite measurements of small-scale deformation.

A second objective was to promote discussion of the following topics:

- Recent progress in small-scale and regional ice–ocean modeling
- Types of ice rheology and yield curves that are optimal for small-scale ice dynamics
- Ice thickness distribution and multi-level ice modeling
- High frequency sea-ice mechanics and simulation of oriented fractures
- Landfast ice and modeling
- Remote-sensed and in situ data for validation of small-scale ice–ocean models

The workshop had four research themes: Sea-Ice Mechanics and Modeling, Sea-Ice Dynamics and Modeling, Small-Scale and Basin-Scale Coupled Ice–Ocean Modeling, and Sea-Ice and Ocean Observations. There were 40 participants (including 32 presentations) from nine countries. Each theme had a rapporteur to chair the discussions and summarize the recommendations at the end of the workshop. The workshop has produced recommendations for small-scale ice–ocean modeling over the next 5–10 years, which will be valuable for MMS needs and be used by IARC-Frontier and the polar research community.

Introduction

In general, most sea-ice models on basin scales use relatively smooth plastic yield surfaces combined with thickness distributions based largely on an aggregate statistical representation of ridging processes. Variable thickness multi-level sea-ice models are typically based on this paradigm, which requires considerable amounts of simultaneous ridging and open water creation to occur under deformation states, involving large amounts of shear but little divergence. While sufficient for pack-ice simulation in the Arctic Ocean for climate study purposes, it is still unclear how to treat and redistribute the spectrum of ice thickness from thin, new ice to thick, ridged ice, and to landfast ice in most of the present models. To accommodate the spectrum of ice thickness, the redistribution is typically carried out in some statistical manner commensurate with the aggregate arguments. These models have not, however, typically considered landfast ice, which observations have shown does evolve in a manner incorporating ridging as it strengthens and extends. Also, a precise manner in which ice is redistributed and what ice classes are used likely needs to be specifically tailored to small-scale models.

Recent studies on small-scale modeling approaches have typically made greater use of fracture-based modeling (including anisotropic models) where rheologies incorporating fracture-based yield curves have been bound to fail with the characteristic formation of intersecting cracks. Aggregate failure characteristics still may be smooth once the initial failure has occurred. Additional issues in small-scale models are rapid kinematic wave propagation (coupling between relative–steady state momentum

1

balances with special changes in the thickness distribution) as ridging fronts move out. High-frequency fluctuation of ice deformation has been a ubiquitous feature of mesoscale strain observed on scales of 5–20 km, under forcing of oceanic inertial oscillation, tides, and storms. These fluctuating effects also put more constraints on a proper numerical solution of coupled ice momentum and thickness equations on a small scale.

Present Progress

Sea-ice modeling

Recent RADARSAT SAR imagery (Figure 1, left panel) shows sea-ice deformation and fractures using Lagrangian elements; the image may show open water, new ice, young ice, first-year and old ice, rafted ice, or ridged ice. Spatial scales of less than 10 km must be used to resolve these features. Furthermore, the shear deformation indicates anisotropic features in sea-ice motion [Kwok 2001]. The new evidence is challenging widely used isotropic sea-ice models that employ viscous-plastic rheology [Hibler 1979]. The small-scale deformation of the RGPS (RADARSAT Geophysical Processing System) dataset provides an impetus toward the advancement of the small-scale modeling effort. However, Hutchings and Hibler [2002] argue that it is possible to simulate intersecting sets of leads with a viscous-plastic sea-ice model and an isotropic rheology when the spatial domain is discretized with sufficiently high resolution. If the sea ice is assumed to be heterogeneous at the grid scale, and allowed to weaken in time, fractures propagate across the region in two preferred directions (Figure 1, right panel).

There are also related unresolved issues in ice–ocean coupling that can particularly affect coastal currents. Most large-scale models, for example, consider the stress transferred into the ocean to be the ocean stress on the lower ice surface, which is relatively smooth spatially and closely mimics the wind stress curl. This paradigm, however, neglects ice convergence, which can significantly modify Ekman fluxes. Simulations considering this by appropriately modifying the stresses into the ice–ocean system as modified by the ice interaction show substantial increases in the Beaufort Sea coastal current.

The major obstacle in development of small-scale and regional sea-ice–ocean models is still a lack of proper verification data. Present satellite data are providing sea-ice velocity fields in high resolution and those products can be used extensively for a verification of ice dynamics. The modeled evolution of sea-ice thickness distribution is practically impossible to verify. However, the forthcoming polar satellites (IceSat, CryoSat) may provide an accurate measurement of ice thickness over a large scale. In reviewing existing data of sea-ice conditions in Arctic coastal regions and future data collection activities, workshop participants identified potential short- and long-term strategies in improving modeling, in particular of coastal landfast ice.

Coupled ice–ocean modeling

Small-scale ice–ocean modeling can capture rich information in the Beaufort–Chukchi seas. Recent simulations using a nested coupled ice–ocean model with an eddy-admitting resolution (3.7 km) in the Beaufort–Chukchi seas [Wang et al. 2002] indicate the necessity of using a fine-resolution model for understanding coastal processes. Figure 2 shows the intercomparison between the simulated sea-ice flow (left) and satellite-observed water color (right) in the study region in August. Mesoscale eddies are clearly captured by both the model and satellite measurement, which cannot be detected in the basin-scale models with coarse horizontal resolution. Furthermore, this model can also capture wintertime Arctic halocline ventilation along the Beaufort–Chukchi coast, probably induced by oceanic upwelling that is driven by the anticyclonic Beaufort Gyre.
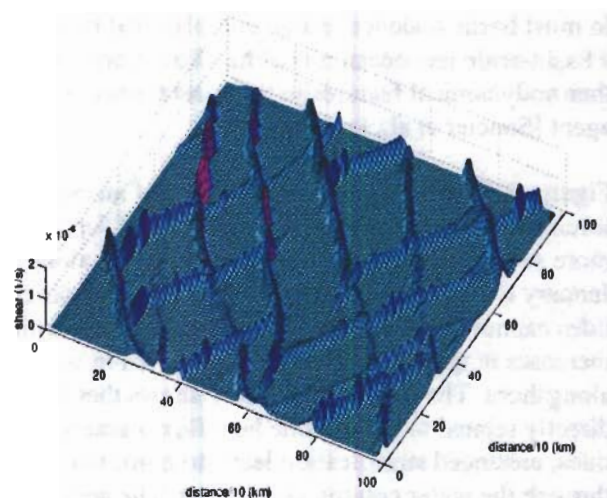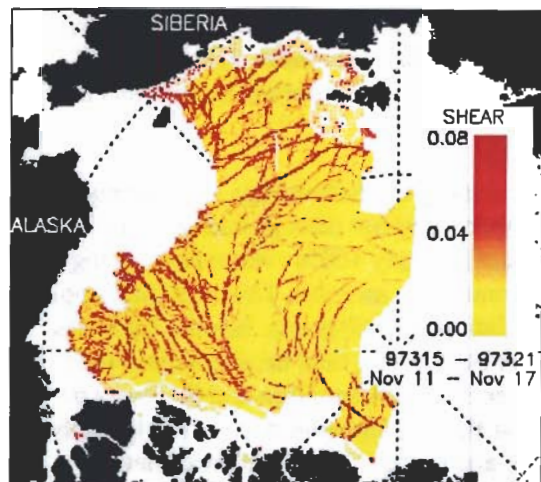
Figure 1. (left panel) Average shear deformation of Lagrangian elements (over six days) with dimensions approximately 10 km × 10 km on a side. The observations are based on small-scale ice motion from the RADARSAT Geophysical Processor System (RGPS). (right panel) Sea-ice shear/fractures as simulated with a viscous-plastic sea-ice model and an isotropic rheology when spatial domain is discretized with sufficiently high resolution.
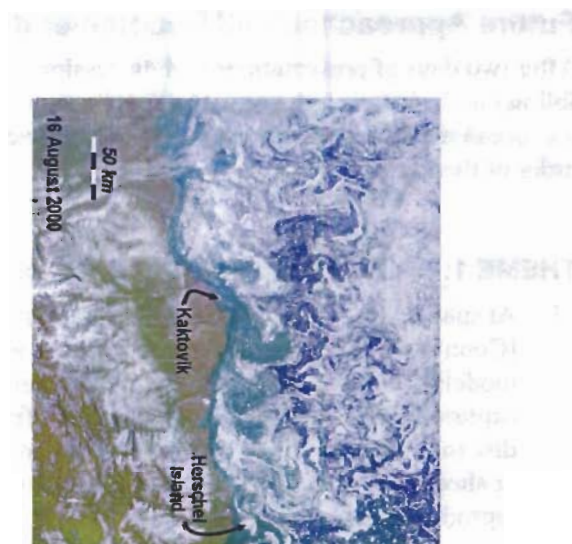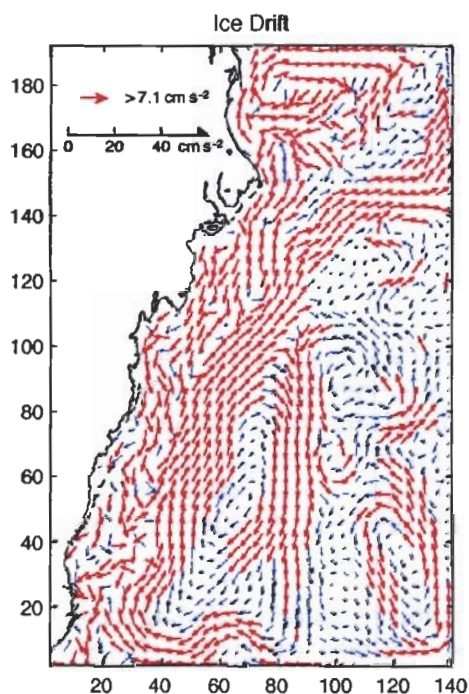
Figure 2. Model-simulated sea-ice velocity (left panel) and satellite-measured water color (right, courtesy of Tom Weingartner, originated from JPL) in the Beaufort–Chukchi seas on 18 August 2000. Mesoscale eddies are visible from the observations, while the model captures an eastward coastal current along the Alaska coast and an offshore westward current. Off the shelfbreak, mesoscale eddies of sea ice are active, similar to the satellite measurement. On the left panel, the axes are labeled by model gridpoint (3.7 km) numbers, so the distance of the x-axis (south to north) is 520 km, while the y-axis (from east to west) distance is 700 km.

3

In most basin-scale ice–ocean models, tidal mixing is simply ignored, which raises concerns of how a basin-scale ice–ocean model handles strong tidal mixing. In simulating ice–ocean dynamical and thermodynamical features in the coastal seas, ocean tides may be the most important mechanical mixing agent [Saucier et al., in press].

Figures 3 shows the seasonal variation of an ocean heat flux anomaly in Hudson Bay, subtracting the tidal forcing solution from the one with no tidal forcing. The simulation without tides produces about 38% more sea ice. The concentration is increased along the coast and is nearly 100% everywhere during the January to April period. Both the averaged thickness and concentration increase. The solution without tides cannot reproduce the obverved polynyas, while the simulation with tides can. Sea-ice thickness increases in the already fully-covered area in southern Hudson Bay, where tidal mixing is important alongshore. The heat flux anomaly shows that the increase in sea-ice concentration and thickness is directly related to the oceanic heat flux, namely a sensible heat flux during wintertime. Clearly, without tides, enhanced stratification leads to more sea-ice production and to the reduction of heat transfer through the water column and sea ice. The sensible heat that was stored in the initial condition remains trapped in the water column. Since tidal mixing is also important in diffusing surface heat at depth during the summer (see the positive heat flux anomaly in summer months of Figure 3), the model could eventually depart from the initial condition and converge into a new steady seasonal cycle without tides, but with a reduced heat cycle and more sea ice. These results also suggest that improvements in the handling of winter convection would not be able to correct the deviation of the no-tide simulation from the observations, as it would not influence the heat transfer to depth in summer.

Future Approaches and Recommendations

After two days of presentations and discussions, the participants were divided into four working groups following the research themes. Major recommendations produced in the workshop for small-scale ice–ocean modeling and observations over the next 5–10 years can be summarized in the following in order of themes:

THEME 1: Sea-Ice Mechanics and Modeling

1. At spatial scales of less than 10 km, satellite observations [Kwok 2001] and theory [Coon et al. 1998] show sea ice to behave in a strongly anisotropic fashion, while most models used to date are isotropic. Thus, anisotropic models should be developed to better capture sea-ice properties such as sea-ice fractures, stresses, ridging, rafting, etc. The discontinuities in the RGPS data should be sorted by type, e.g., shear, shear with opening, or shear with closing. It is useful to use Kwok's data to determine if isotropic models reproduce types of features.

2. Landfast ice is crucial to coastal processes. Thus, landfast ice models including scouring and anchoring processes should be developed. At the same time, parameterization of landfast ice in a coupled ice–ocean model may be the initial step. The processing of the RGPS data should be extended to shore for use in the validation of fast-ice models.

3. For climate atmosphere–sea-ice–ocean models with grid sizes larger than 10 km, a parameterization of processes at the 10-km scale is necessary to capture anisotropic behavior. At 100-m resolution, continuum models are unlikely to work; thus, discrete (Lagrangian) models are needed. Fine resolution continuum models (~1 km) should be used.

4

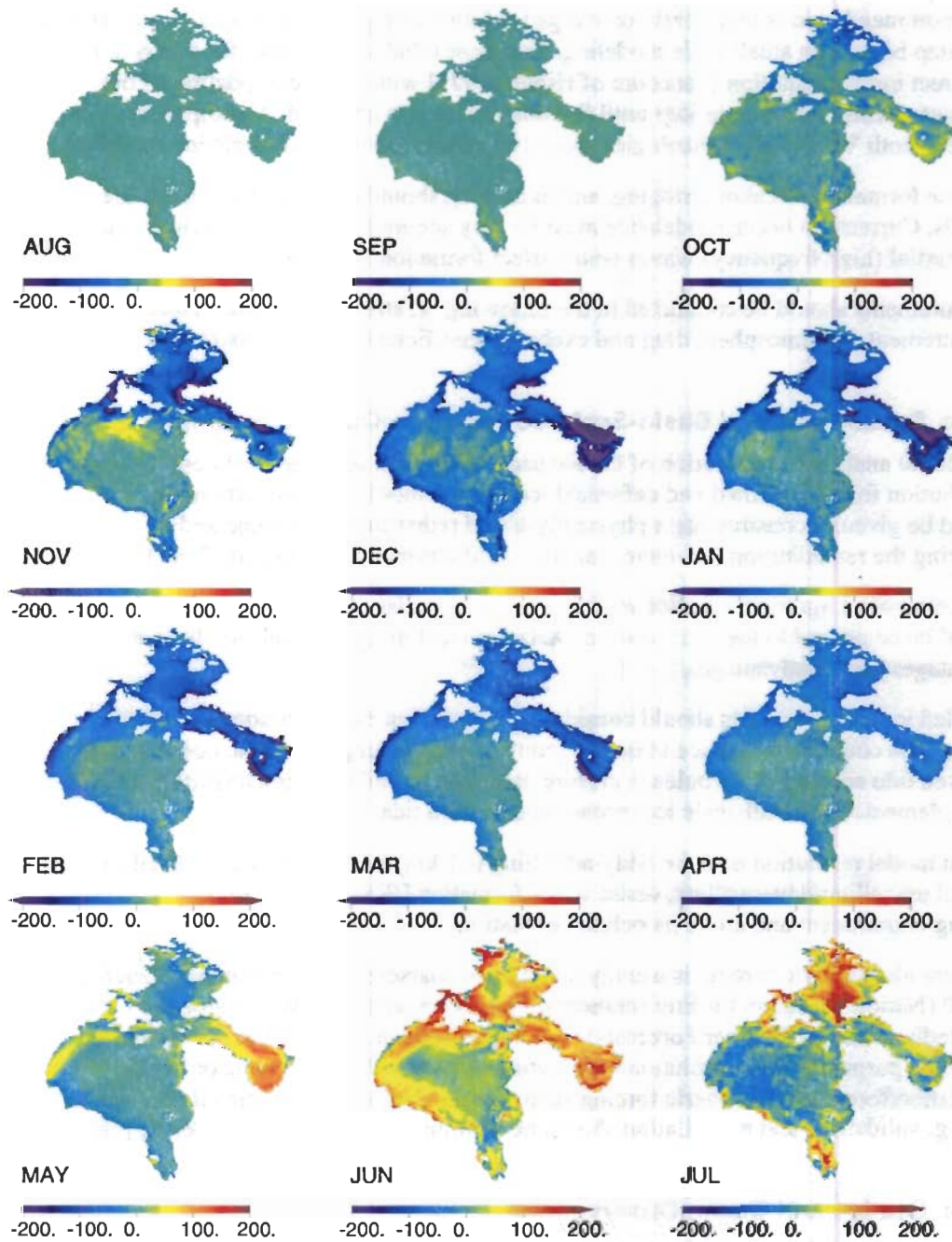Figure 3. The oceanic heat flux anomaly without tides (the solution with no tides minus the one with tides) in Hudson Bay, simulated by a coupled ice–ocean model. Units are in W m^{-2}. A positive value indicates stronger heat flux released by tidal mixing and a negative value indicates less heat flux exchange between the water column and sea ice because more sea ice (higher concentration and thickness) is produced.

THEME 2: Sea-Ice Dynamics and Modeling

4. Although the elastic-viscous-plastic solution [Hunke and Dukowicz 1997] of the viscous-plastic [Hibler 1979] sea-ice model is generally good for large scale climate modeling, the recommendation is that a fully converged solution of the viscous-plastic model at each time step be used in small scale modeling. The most reliable procedure for this is to use the direct implicit solution procedure of Hibler [1979] with repeated updating of the nonlinear terms at each time step until full convergence is obtained. A comparison between both VP and EVP rheologies should be conducted on small-scale ice modeling.

5. Fast-ice formation, breakout, ridging, and anchoring should be studied using sea-ice models. Currents in ocean models/ice must be very accurate for coupling. Kinematic and inertial (high frequency) waves could affect formation location.

6. Measurements should be conducted in the following: a) stress and strain, b) direct measurements of atmosphere drag and exchange coefficients, and c) topography.

THEME 3: Small-Scale and Basin-Scale Coupled Ice–Ocean Modeling

7. In order to analyze the evolution of the ice pack in detail, a separate thickness distribution for undeformed and deformed ice classes should be used. Attention should be given to constructing a physically-based redistribution scheme and to verifying the redistibution parameters against field observations [Haapala 2000].

8. Discontinuous Lagrangian sea-ice models such as granular models [Hopkins 1996] should be compared to the continuum models such as Eulerian models to elucidate advantages and disadvantages.

9. Coupled ice–ocean models should consider mixing driven by ocean tides and surface waves. The coupling of sea-ice stress and convergence/divergence to the ocean should be taken into account. A turbulence closure model or a similar parameterization should be implemented in small-scale ice–ocean models with tidal forcing.

10. Ocean model resolution must be eddy-admitting (~1 km) to resolve mesoscale eddies, coastal upwelling/downwelling, dense water formation [Wang et al. 2002], mixing/entrainment and arctic halocline ventilation.

11. Because atmospheric forcing is usually taken from coarse-resolution reanalysis such as NCEP (National Centers for Environmental Prediction) and ECMWF (European Centre for Medium-Range Weather Forecasts) reanalysis products, for small-scale ice–ocean modeling purposes, high-resolution observations and reanalysis products or MM5 simulation/forecast atmospheric forcing fields are needed. An observational plan for forcing, validation, and assimilation should be well integrated with the modeling plan.

THEME 4: Sea-Ice and Ocean Observations

12. Observational studies should be conducted to collect data in:

   Regional atmosphere parameters
   Regional meteorological analyses (data assimilation)
   Surface energy balance
   Melt pond convergence
   Albedo
   Snow accumulation

Coastal ocean
Sediments/entrainment/transport
Association with storms
River input (overflow, flux)
Hydrography (fronts, current, ocean structure etc.)
Sea level
Bathymetry

Sea ice
Fast ice – stability, coverage
Fast ice thickness profile (laser profiler)
Fast ice deformation (radar interferometry)
Ice motion (RADARSAT, others)
Sediments/contamination (Modis, Landsat) coverage
Local sea-ice thickness distribution

Thus, it is recommended that:

1. Coastal RADAR is needed.

2. Connections to synoptic and basin scale dynamics should be emphasized, such as coupling between the large-scale pack ice and landfast ice.

3. Critical parameters should be identified, such as fast ice breakout, ridging, formation, thickness, melt ponds, etc.

4. A science dataset for coastal ocean should be archived.

SIOM Working Group Recommendations (recorded by rapporteurs)

THEME 1: Sea-Ice Mechanics and Modeling

Landfast ice
The following issues need to be addressed. Where does oil in ice go? Where does ice go? What are the time scales of breakup, from hours to days? What are the relationships between breakup and cracks, and river runoff?

Pack ice
1. Pack ice can push fast ice into shore. Thus, pack ice can provide boundary conditions for landfast ice models/calculations.

2. What is pack ice modeling scale? If at 10 km, Ron Kwok's data shows many inactive regions, which allows resolution of rigid and deforming regions and is good for BCs.

3. What is the timescale for a pack model? If using a 6-hr atmospheric forcing or coupling timescale (e.g., NCEP reanalysis), it is not interested in a 10-min timescale of lead formation. So, the wind forcing (hourly wind can resolve sea breezes) decouples with lead formation of timescale of 10 min (i.e, sea-ice internal mechanics determines its lead and cracks, given hourly wind and thermodynamical forcing.

Isotropic or anisotropic?

Isotropy → Characteristics are features on >10 km spatial/length scales? Features visually are similar to data.

It is recommended that:
1. Use Kwok's data to determine if isotropic models reproduce types of features.

   Because physical arguments on 10 km suggest anisotropy, we need to test
   • Discrete element, anisotropy models (Mark Hopkins)
   • Continuum, anisotropy models (Climate timescales?)

   using parameterization of 10 km processes for anisotropic climate models.

2. Ron Kwok's data in near shore should be processed.

3. Many thickness levels? With absence of data, is it *computationally* worthwhile? (As opposed to scientifically?)

4. Use field data and discrete simulations to help anisotropic thickness distribution.

Inshore ice

1. Finer resolution of continuum models *~1 km.*

2. More points/floes in discrete model.

3. Capture fixing points and rounded keels. Oil industry would like 1 m, the limit of continuum assumption. Basal slope 20 m/5 km.

4. At 100-m resolution, continuum models unlikely to work. Need discrete model.

Timescale, limited to:

1. Break-out and freeze-up events—hours to days (6 hours)

2. Tides (3 hours)
   Because breakout is important for oil transport and pack ice (arching) thickness

3. Force and deformation data are needed on ~100 m
   Lengthscales to test/calibrate models

4. Does oil industry have these fine-resolution data? Is it easy to get?
   Extent of landfast ice from Landsat/AVMRR imagery

5. Atmospheres/ocean forcing resolution for ice models?
   Pack forces > atmosphere forces
   Thermal forces great
   Thermodynamic considerations are more important

THEME 2: Sea-Ice Dynamics and Modeling

The following issues should be addressed:
1. Formation of fast ice (ridges, gouging, destroying pipelines)

2. Tidal currents, fast ice can affect motion, erosion, deposition, sediment transport, break away of fast ice, particularly during spring time—high tide.

3. Strengthening of ridges (diffusion process, salinity increase)

4. Coupling effects of current with fast and pack ice: formation and breakout

5. River outflow on breakup

8

6. Turbulent effects of eddies and geophysical scouring formation of fast ice

7. Movement of fast ice 0.5 km—smaller

8. 3D Problem—ridge variation with height

9. Anchoring and soil mechanics

Modeling
1. Currents in ocean models/ice must be very accurate

2. Kinematic and inertial (high frequency) waves could affect formation location

Measurements
1. Stress and strain measurements

2. Direct measurements of atmosphere drag and exchange coefficients

3. Topography

THEME 3: Small-Scale and Basin-Scale Coupled Ice–Ocean Modeling

Research plan for small scale near shore sea-ice–ocean–land–atmosphere modeling:
1. The learning of small scale processes directly improves basin scale understanding

2. Basic tools exist to tackle 1 to 10 km scales, but important issues remain:
   - Rheology* and Eulerian vs. Lagrangian approach
   - Fluxes and turbulence, boundaries, drags, etc.
   - Need for including several new processes, e.g., melt ponds, flooding, freshwater trapping, salt separation rates, new fast ice category, etc.
     *= Elasticity? Ansiotropy?

3. Major model components need to be added for waves, surges and tides.

4. Models should pay more attention to propagation of errors in forcing or parameters onto P.D.F. solutions (ensemble runs, etc.)

5. The knowledge of forcing is more limiting than the knowledge of the physics

Bi-directional nesting with O (1 km) will include eddies, thin layers, coastal currents, mixing and entrainment
1. An observational plan for setup, forcing, validation, and assimilation should be well integrated with the modeling plan.

2. Assimilation methods not violating conservation laws.

Observational requirements:
1) Model setup, 2) Forcing, 3) Validation, 4) Assimilation, and
5) Empirical studies to sub-grid parameterizations

1. Topography < 1km in the horizontal, ~10 cm in the vertical, repeated over time. Further analysis for evolution (scour, sediment transport, grain size).

2. Combine atmospheric data with large-scale re-analysis (MM5, downscaling) including higher moments. May need new data? Precipitation? Winds over sea? Runoff, roughness.

3. Ice motion and deformation, internal stress, ridges, ice/snow thickness—through the season as possible! Ocean currents, 3-D fronts, T, S, TKE, E (fine structures).

4. Ice thickness, ocean fronts, MLD (mixed layer depth), salinity, remote sensing data, budget conserving schemes is an important issue.

5. See above list.

THEME 4: Sea-ice and Ocean Observations

- Short Term: 2002–2007
- Geographic focus: Beaufort (Chukchi, Cook Inlet, Norton Sound)
- Objectives:
    - Support of model forcing, development, validation/assimilation
    - Development of climatology, process studies
    - Monitoring of processes
    - Connection to larger scale climate
    - Time scale: daily, monthly, interannual and decadal

Regional atmosphere
- Regional meteorological analyses (data assimilation)
- Surface energy balance
    - Land/ice interactions (differential responses and coupling)
    - Melt pond converge
    - Sediments – albedo
    - ARM
- Meteorological stations (concern)
    - Snow accumulation

Coastal ocean
- Sediments/entrainment/transport
    - association with storms
- River input (overflow, flux)
- Hydrography (fronts, current, ocean structure etc)
- Sea level
- Bathymetry

Coastal ocean
- Fast ice – stability, coverage
- Fast ice thickness profile (laser profiler)
- Fast ice deformation (radar interferometry)
    - Model-based interpretation
- Ice motion (RADARSAT, others)
    - Local smaller scale observations
- Sediments/contamination (Modis, Landsat)
    - Coverage
- Local sea-ice thickness distribution

Recommendations
- Coastal RADAR!! – Connections to synoptic and basin scale dynamics
- Identification of critical parameters
- Repository/archive for science dataset for coastal ocean

Acknowledgements

References

Coon, M.D., G.S. Knoke, D.C. Echert and R.S. Pritchard. 1998. The architecture of an anisotropic elastic-plastic sea ice mechanics constitutive law, J. Geophys. Res. 103:2191521925.

Haapala, J. 2000. On the modelling of ice-thickness redistribution. J. Glaciology 46:427437.

Hibler III, W.D. 1979. A dynamic thermodynamic sea ice model, J. Phys. Oceanogr. 9:815–846.

Hopkins, M.A. 1996. On the mesoscale interaction of lead ice and floes. J. Geophys. Res. 101:18315–18326.

Hunke, E.C., and J. K. Dukowicz. 1997. An elastic-viscous-plastic model for sea ice dynamics. J. Phys. Oceanogr. 27:1849–1867.

Hutchings, J.K., and W.D. Hibler III. 2002. Modeling sea ice deformation with a viscous-plastic isotropic rheology, p. 358–366. *In* V.A. Squire et al. [eds.], Proceedings of the 16th International Symposium on Ice, International Association for Hydraulic Engineering and Research, Vol. 2. 2–6 December 2002, Dunedin, New Zealand.

Kwok, R. 2001. Deformation of the Arctic Ocean sea ice cover: November 1996 through April 1997, p. 315–323. *In* J. Dempsey and H.H. Shen [eds.], Scaling Laws in Ice Mechanics and Dynamics. Kluwer Acadmic.

Saucier, F.J., F. Roy, D. Gilbert, P. Pellerin and H. Ritchie. In press. The formation and circulation processes of water masses in the Gulf of St. Lawrence. J. Geophys. Res.

Wang, J., M. Ikeda and F.J. Saucier. 2003. A theoretical, two-layer, reduced-gravity model for descending dense water flow on continental slopes. J. Geophys. Res. 108(C5), 10.1029/2000JC000517

Wang, J., Q. Liu and M. Jin. 2002. A nowcast/forecast model for the Beaufort Sea ice–ocean–oil spill system (NFM-BSIOS), p. 80–94. *In* University of Alaska Coastal Marine Institute Annual Report No. 8. OCS Study MMS 2002-001, University of Alaska Fairbanks and USDOI, MMS, Alaska OCS Region.
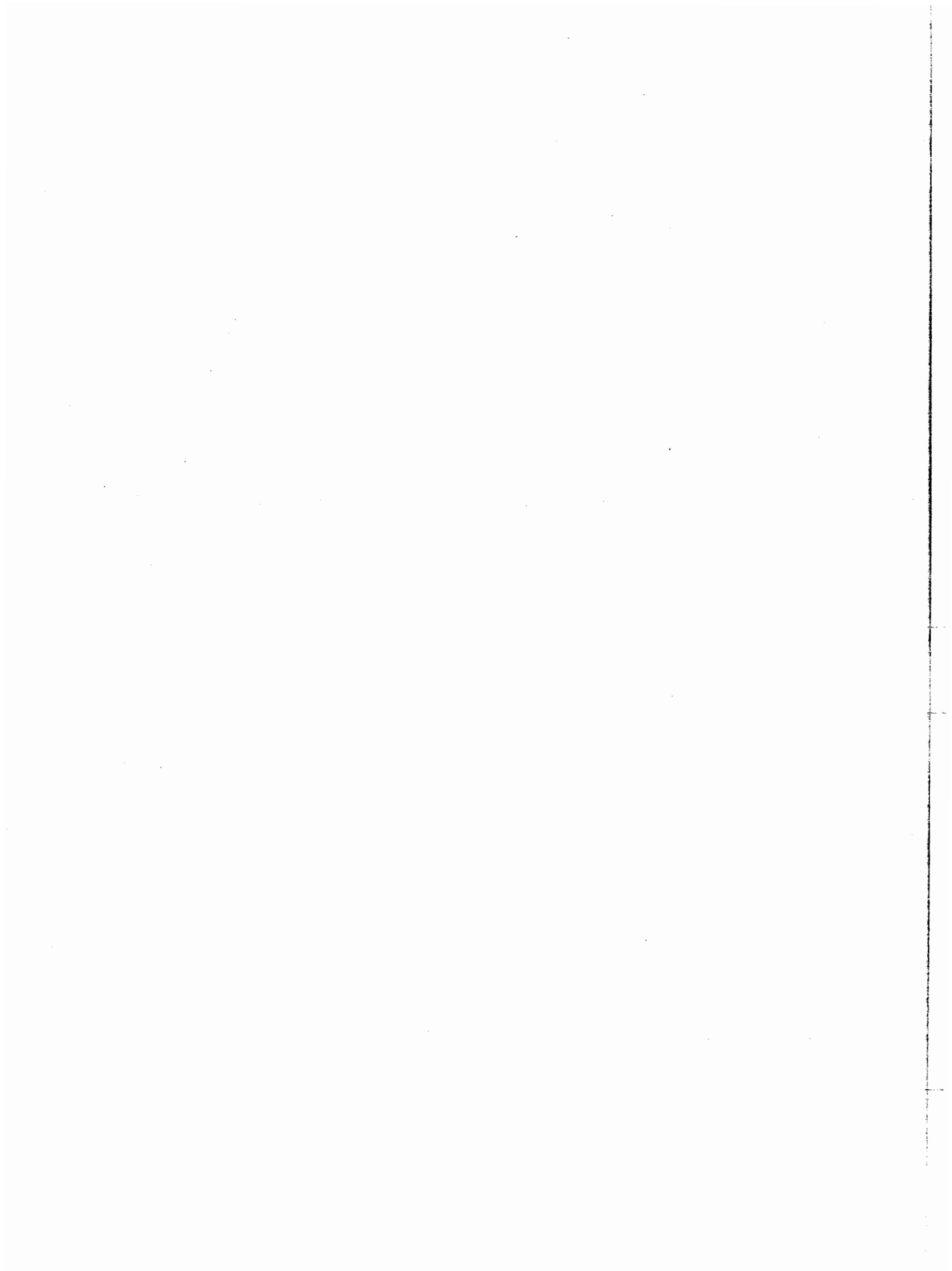
Workshop Agenda

SIOM (Small-Scale *Sea Ice* and *Ocean Modeling*)
AUGUST 7–9, 2002
International Arctic Research Center
Fairbanks, Alaska

Wednesday, August 7

8:30–9:00:   Continental breakfast, IARC room 401

9:00–9:30:   Opening remarks, Introductions, Orientation to Fairbanks
                Jia Wang   Workshop Chairman
                Paul Reichardt   Provost of UAF
                Syun Akasofu   Director of IARC
                Vera Alexander   Dean of SFOS and Director of CMI
                Moto Ikeda   Dean of GSEES, Hokkaido University and Advisor
                                      (Former Program Director) of IARC-FRSGC

9:30–9:50:   "Workshop Expectations: MMS Perspectives" by MMS Program Manager,
                Richard Prentki, Ph.D.

Theme 1 Chair: Moto Ikeda (Sea Ice Mechanics and Modeling)
(invited: 30 mins, others: 20 mins, posters: 5 mins)

9:50–10:40:   Presentations from Theme 1
        ◆Jari Haapala: "Open Questions of Calculation of Redistribution of Sea-Ice" (invited)
        ◆Max Coon: "Pack Ice Anisotrophic Constitutive Law"

10:40–11:00: Coffee break

11:00–12:50: Presentations from Theme 1 (continued)
          ◆Mark Hopkins: "High-resolution Arctic Basin Sea Ice Modeling"
          ◆H.L. Schreyer: "An Application of the Material Point Method to Oriented
                                        Failure of Sea Ice"
          ◆Daniel Feltham: "A Continuum Rheology of Anisotrophic Sea Ice"
          ◆Robert Pritchard: "Fast Ice Dynamics and Anisotropic Plasticity"
          ◆Bill Hibler: "On Simulating Oriented Failure Zones in Sea Ice Velocity
                                        Fields" (poster presentation, 5 mins)

12:50–1:00:   Group Photo
                Front steps of IARC Building

1:00–2:00:   Lunch, IARC 5th floor

2:00–3:00:   Discussion of Theme 1
                Rapporteur: Max Coon

Theme 2 Chair: Markus Meier (Sea Ice Dynamics and Modeling)

3:00–3:50:   Presentations from Theme 2
      ♦Bill Hibler: "Scale Invariant Sea Ice Dynamics for Small Scale Sea Ice
                             Models" (invited)
      ♦Bin Cheng: "Modeling of Superimposed Ice Freezing and Sub-Surface
                             Melting Based on BASIS98 and BASIS99 Data"

3:50–4:10:   Coffee break

4:10–5:50:   Presentations from Theme 2 (continued)
      ♦Jennifer Hutchings: "Modelling Observed Sea Ice Deformation in the Western Arctic"
      ♦Petteri Uotila: "An Impact of Sub-grid-scale Ice–Ocean Dynamics on Sea-Ice Cover"
      ♦Leif Pedersen: "Applications of a Marginal Ice Zone Model"
      ♦Keguang Wang: "On the Formation and Orientation of Leads and Ice Ridges"
      ♦Denis Zyryanov: "Mechanical Simulation of Shorefast Ice Break-up: Kara and Laptev Seas"

5:50–6:30:   Discussion of Theme 2
                Rapporteur: William Hibler

7:30–9:00 p.m.: Reception at the Pike's Landing
(bus transportation to Pike's Landing at 7:10 p.m. and back to Campus at 9:00 p.m.)

Thursday, August 8

8:30–9:00:   Continental breakfast, IARC 401

Theme 3 Chair: Jari Haapala (Small-Scale and Basin-Scale Coupled Ice–Ocean Modeling)

9:00–10:50:   Presentations from Theme 3
      ♦Moto Ikeda: "Parameterization of Thin Ice in a Coupled Ice–Ocean Model: Application
                             to the Seasonal Ice Cover in the Sea of Okhotsk" (invited)
      ♦Quizheng Liu   "Sea Ice Modeling for the Bohai Sea of China"
      ♦William Garwood: "Thermodynamics Critical to Arctic Mixed Layer Systems"
      ♦Jia Wang: "A Nested Coupled Ice–Ocean Model for the Beaufort Sea"
      ♦Keguang Wang: "A Numerical Investigation of Sea Ice Dynamics in the
                             Gulf of Riga" (poster introduction, 5 mins)

10:50–11:10: Coffee break

11:10–12:30: Presentations from Theme 3 (continued)
      ♦François Saucier: "Modelling the Formation and Circulation Processes of
                             Water Masses and Sea Ice in the Gulf of St. Lawrence, Canada (invited)
      ♦Xiangdong Zhang: "Coordinated Changes of Sea-ice and Ocean Properties in the Beaufort
                             and Chukchi Seas"
      ♦Wieslaw Maslowski: "Modeling the Arctic Ocean and its Sea Ice: From a Local
                             to Basin Scale"
      ♦Meibing Jin: "A Coupled Ice–Ocean Model in the Pan Arctic and North Atlantic
                             Ocean: Seasonal Cycle"

♦Bin Cheng: "The Impact of Numerical Resolution on Predictions of a Thermodynamic Sea Ice Model" (poster introduction, 5 mins)

12:50–2:00: Lunch, IARC 5th floor

2:00–2:45: Presentations from Theme 3 (continued)
♦Markus Meier: "On the Sensitivity of Baltic Sea Ice Variability to the Changing Climate"
♦Jing Zhang/ "Towards Accurate Sea-Ice Modeling in a Coupled MM5/Sea-Ice Model:
  Jeffrey Tilley: Treatment of the Ocean"
♦Bin Cheng: "Modeling of Sea Ice Thermodynamics and Air–Ice Coupling During Warm Air Advection" (5 mins)

2:45–3:40: Discussion of Theme 3
Rapporteur: François Saucier

3:40–4:00: Coffee break

Theme 4 Chair: Hajo Eicken (Sea Ice and Ocean Observations)

4:00–6:00: Presentations from Theme 4
♦Ron Kwok: "Small-Scale Kinematics from RADARSAT SAR Imagery" (invited)
♦Andrew Mahoney: "Small-Scale Fast Ice Processes: Implications for the Coastal Regime and Large Scale Models"
♦Boris Ivanov: "Peculiarities of the Vertical Temperature and Salinity Water Structure in the Melt Ponds on the Land Fast and Drifting Ice"
♦Lewis Shapiro: "The Importance of the Interactions between Landfast Ice and Pack Ice for Models of the Nearshore Chukchi and Beaufort Seas"
♦Nori Tanaka: "Reevaluation of Water Mass Tracers in the Arctic Ocean"
♦Igor Appel: "Experience of Supporting Users with Specialized Information on Ice over State" (poster presentation, 5 mins)

7:00 p.m. Bus transportation to Tanana Valley Fair. Meet in front of Natural Science Building. Return transportation will be from main fairground entrance at 9:00 p.m. and 9:30 p.m.

Friday, August 9

8:30-9:00: Continental breakfast, IARC 401

Theme 4 Chair: Ron Kwok (continued)

9:00–10:00: Presentations from Theme 4 (continued)
♦Hajo Eicken: "Observations and Modeling of Small-Scale Thermodynamic Ice Growth and Decay Processes in Coastal Arctic Seas" (invited)
♦Aleksey Marchenko: "On the Excitation of Natural Shelf Modes due to Self- Induced Oscillations of Ice Floes by Ridges Buildup"
♦Kazutaka Tateyama: "Introduction of Sea Ice Monitoring Radar Network on the Okhotsk Coast of Hokkaido"

10:10–11:00: Discussion of Theme 4
                Rapporteur: Ron Kwok

11:00–11:20: Coffee break

11:20–12:50: Working group meeting to finalize the recommendations that each theme contributes:

		IARC Room
Theme 1 (Sea-Ice Mechanics and Modeling):	Max Coon	407
Theme 2 (Sea-Ice Dynamics and Modeling):	Bill Hibler	417
Theme 3 (Small-Scale and Basin-Scale Coupled Ice–Ocean Modeling):	François Saucier	401
Theme 4 (Sea-Ice and Ocean Observations):	Ron Kwok	5th floor

12:50–2:00: Lunch, IARC 5th floor

2:00–3:00: Working group meeting (continued):

Theme 1 (Sea-Ice Mechanics and Modeling):	Max Coon
Theme 2 (Sea-Ice Dynamics and Modeling):	Bill Hibler
Theme 3 (Small-Scale and Basin-Scale Coupled Ice–Ocean Modeling):	François Saucier
Theme 4 (Sea-Ice and Ocean Observations):	Ron Kwok

3:00–5:00: Plenary session and summary by rapporteurs of Themes 1–4 (Chair: Jia Wang)

Max Coon	(15 min)
Bill Hibler	(15)
François Saucier	(15)
Ron Kwok	(15)
Jia Wang	(15) closing the plenary session

6:10–9:30 p.m.:	Workshop Dinner, River's Edge Resort
6:10 p.m.:	Bus departs from Natural Sciences Building
6:30 – 7:30 p.m.:	Appetizers and No Host Bar
7:00–7:30 p.m.:	Invited speech: "The Mystery of the Aurora" by Dr. Syun Akasofu, chaired by Dr. Nori Tanaka, IARC/FRSGC, Acting Program Director
7:30–9:30 p.m.:	Dinner
9:30 p.m.:	Bus transportation to Cutler Apartments

Workshop Abstracts

THEME 1: Sea-Ice Mechanics and Modeling

Open Questions of Calculation and Redistribution of Sea-Ice

JARI HAAPALA
Department of Physical Sciences, University of Helsinki

A typical pack ice field is a mixture of open water, undeformed and deformed ice classes of variable thickness. In general, the pack ice is described by the ice thickness distribution function and its evolution is determined by the horizontal advection, thermodynamical growth and decay and a redistribution of ice. The most unknown term in this equation is the redistribution term, which describes physically in a continuum scale. How the small scale deformations occur depends on the large scale strain rates, which ice thicknesses experience deformations, and what is a typical shape for a deformed ice. These questions were already discussed in depth during the AIDJEX program, but since which very little progress has been done. For example, present numerical models that resolve ice thickness redistribution and possibilities to utilize present and future satellite data for a more comprehensive analysis of the redistribution of pack ice are revisited.

Numerical experiments are presented in order to test a sensitivity of a modeled ice thickness field for various ice redistribution schemes. Sea ice thickness distribution is discretizated for five thickness categories of undeformed ice and two single thickness categories of deformed ice. Thermodynamic growth rates and drag coefficients are inherent for each ice class and category. The model employs a curvilinear coordinate, which allows simulation of mesoscale dynamics in coastal regions of the Arctic Ocean. These areas are known to be the vital regions for sea ice deformations.

Pack Ice Anisotropic Constitutive Law

MAX COON

The two striking facts about present ice dynamics models are that they do not: 1) reproduce the oriented fracture patterns of openings and closings in the pack, and 2) accurately model the effects of frazil/pancake ice formation in the ice margin. These are areas that produce the most ice growth, the most turbulent heat flux to the atmosphere, the most salt flux to the ocean, and the most energy dissipation due to slippage, ridging, and rafting. The first shortcomings will be addressed here. Existing sea ice models have shown limited success for predicting the degree to which any given lead will open for prescribed or even observed forcing conditions.

An anisotropic plastic rheology introduced by Coon et al. [1992,1998] described the opening of leads associated with traction free lines that can admit discontinuities in displacement. Anisotropic constitutive law for use in the sea ice dynamics model is presented here. This accounts directly for refrozen lead systems in the pack ice strength (with anisotropic failure surface) and in the ice thickness distribution (with an oriented thickness distribution). The lower limit (5 km) of the model resolution is controlled by the fracture spacing of old, thicker ice and the maximum lead width. The upper limit of the model resolution (100 km) is controlled by curvature in the lead directions and variations in lead width. These, in turn, are controlled by the variations in internal ice stress due to driving forces (wind and currents), which set the time resolution. In addition, the principal stress normal to a new lead must be zero as it happens. This

model can have subscale parameterizations that allow for the inclusion of phenomena such as ridging, rafting, buckling, and fracture on the behavior of ice.

Coon, M.D., G.S. Knoke, D.C. Echert, and R.S. Pritchard, The architecture of an anisotropic elastic-plastic sea ice mechanics constitutive law, Journal of Geophysical Research, 103(C10), 21915-21925, 1998.

Coon, M.D., Echert, D.C., and Knoke, G.S. (1992), Pack Ice Anisotropic Constitutive Law, IAHR 92, Proceedings of the 11th International Symposium on Ice, Banff, Alberta.

High-Resolution Arctic Basin Sea Ice Modeling

MARK A. HOPKINS
US Army Corps of Engineers ERDC-CRREL, 72 Lyme Rd., Hanover, NH

The ice pack covering northern seas is composed of a mixture of thick ridged and rafted ice, undeformed ice, and open water. Existing ice-ocean models of the Arctic ice pack are large-scale Eulerian continuum models that use a plastic yield surface to characterize the constitutive behavior of the pack. An alternative is to adopt a discontinuous Lagrangian approach and explicitly model ice parcels and the interactions between them. I have developed a granular model of the central Arctic ice pack that consists of tens of thousands of individual floes. Neighboring floes can freeze together to form frozen viscous-elastic joints that can fracture. Each floe has its own thickness distribution. A multi-layered, one-dimensional thermodynamic model is used to simulate melt and growth in each thickness category. Wind stress and temperature fields and Coriolis accelerations drive the model pack. Simulations begin with all floes in the model pack frozen together and at rest. As the floes accelerate in response to the wind, fractures are initiated throughout the model pack and coalesce to form a fracture pattern that covers the basin. The fracture pattern defines many large plates that are composed of aggregates of the basic, small floes. Subsequent deformation takes place along the boundaries of the aggregates. Regional variations in the size of the aggregates correspond to regional variations in the gradient of the wind field and the thickness distribution. Once the joint between two floes has broken they can separate to form leads or be pushed together to form pressure ridges. Pressure ridging is incorporated via a parameterization based on discrete element simulations of the ridging process. At the end of each 24-hour period the model pack is reinitialized. Reinitialization begins by placing an undeformed configuration over the deformed pack. The thickness distribution in the deformed pack is passed to the undeformed pack. New ice is grown in leads. The undeformed pack is run for one hour to create a new aggregate fracture pattern and to equilibrate the stress and velocity fields to the new daily wind field. The model is used to run simulations of several months duration. The simulation results are compared to the maps of Linear Kinematic Features (LKFs) produced by the Radarsat Geophysical Processor System (RGPS). The output of the model pack is run through a virtual RGPS to generate similar maps of LKFs to use in the comparison. Regional variation of the basic floe size permits high resolution (~1 km) simulation of areas of interest.

An Application of the Material Point Method to Oriented Failure of Sea Ice

H.L. SCHREYER[1] AND D.L. SULSKY
[1]*Department of Mechanical Engineering, Department of Mathematics and Statistics, University of New Mexico, Albuquerque, NM 87131*

Failure of sea ice, as exhibited through the formation of leads, is one of the dominant modes of behavior that must be captured if the motion of sea ice is to be modeled successfully. The use of a discrete constitutive equation to represent the evolution of decohesion is conceptually much simpler than using fracture mechanics or failure criteria based on continuum constitutive equations. Criteria for failure initiation can be proposed and checked directly instead of using an indirect approach involving large deformations in

a small zone as predicted through the use of continuum models for plasticity or viscoplasticity. The use of continuum constitutive equations for predicting failure often leads to ill-posedness, an aspect not present with the use of a decohesive constitutive equation. Furthermore, when the decohesive and continuum constitutive equations are solved simultaneously, the resulting algorithm is as simple as that for conventional plasticity so there is no loss in computational efficiency when the decohesive formulation is applied.

Because of the large local deformations associated with material failure, the numerical aspects of the problem remain daunting. Here, we propose to use a new numerical technique, called the material-point method (MPM), which has unique properties that make it particularly amenable to predicting material failure. MPM uses two representations of the continuum being modeled. First, a set of material points (or particles) is identified in the body of fluid or solid that is tracked throughout the deformation process. Each material point has a mass, position, velocity and stress, as well as material parameters and internal variables as needed for constitutive models or thermodynamics. These material points provide a Lagrangian description of the material that is not subject to mesh tangling because no connectivity is assumed between the points. This Lagrangian frame models convection and transport naturally since the trajectory and history of each material point is followed. Each point carries material properties without error and history variables necessary in constitutive models, including the discrete one, can be integrated along the trajectory. An Eulerian frame in the form of a regular, background mesh that covers the computational domain is also introduced. Information is transferred from the material points to the background mesh, the momentum equation is solved on the background mesh, and then information from the mesh solution is used to update the material points. This completes a typical cycle.

In this presentation, a brief discussion of the constitutive formulation and the material point method is given. In addition, solutions to model problems are provided to indicate that failure across element boundaries can be tracked with no modifications to the basic algorithm. The foundation is therefore established for efficient, large-scale analyses in which additional features such the freezing of open leads, the closing of existing leads with ridge formation, and variable ice thickness can be taken into account.

A Continuum Rheology of Anisotropic Sea Ice

ALEXANDER WILCHINSKY AND DANIEL FELTHAM
Centre for Polar Observation and Modelling, Dept. Space and Climate Physics, UCL, UK
email: daniel.feltham@cpom.ucl.ac.uk

Sea ice dynamicists during AIDJEX[1], and most subsequent researchers, have postulated that, in the inelastic regime, the internal ice stress tensor s_{ij} be a function solely of the velocity deformation tensor $\partial u_i/\partial x_j$ and scalars. The requirement of material frame indifference[2] then implies that

$$\sigma_{ij} = \sigma'_{ij} = 2\eta \,\&_{ij} +[\zeta - \eta] \,\&_{ij}\,\delta_{ij} - \tfrac{1}{2}P\delta_{y} + \gamma \,\&_{ik}\,\&_{ij} \tag{1}$$
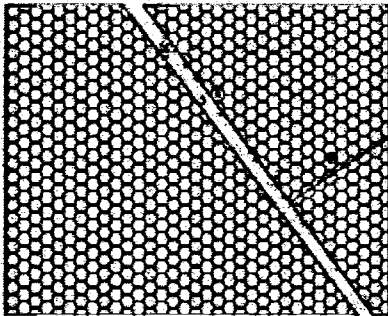
where $\&_{ij} = \tfrac{1}{2}(\partial u_i/\partial x_j + \partial u_j/\partial x_i)$ is the strain rate; η, ς are shear and bulk viscosities and P is ice strength; η, ς and P are functions of the strain rate invariants and scalars. Equation (1) is the general Reiner-Rivlin constitutive relation, which is isotropic; in sea ice models, γ is set to zero. This general form allows plastic or viscous behaviour depending upon the functional form of the viscosities, as in Hibler's well-known, and widely implemented, viscous-plastic rheology[3]. The isotropy of this rheology is generally justified where one resolves length scales of order 100 km and greater as the distribution of oriented features (e.g. cracks, leads, ridges) on this scale is, on average, isotropic. We, however, are interested in resolving physical processes on length scales of order 1–100 km so that we can develop a rheology more appropriate for smaller-scale, potentially anisotropic sea ice dynamics. We allow the stress tensor to depend upon the

19

presence of linear regions of thin ice (*flaws*) embedded in an, otherwise, homogenous ice cover of constant thickness. A flaw is characterised by two vectors: r (and b), with magnitude equal to the thickness *h* (width *w*) of the ice in the flaw and whose direction is normal n (tangent δ) to the flaw, see figure.

The distribution of flaws is given by a function $\varphi(t,x,r,b)$ which is the probability of finding a flaw characterised by r and b at position x and time *t*. The position x is the centroid of a representative area element (an area containing a representative mixture of ice types). We allow the influence of the anisotropy of the flaw distribution to affect the internal ice stress through the weighted, second moment of the vector r,

$$R = \langle r \otimes r \rangle - \int \phi r \otimes r \, dr \, db \qquad (2)$$

where $\otimes$ denotes the dyadic (tensor) product. The quantity R also appears in the theory of polymer suspensions, where it is known as the *structure tensor*.

We propose a bilinear dependence of anisotropic stress $\sigma_{ij}^{\wedge}$ upon the structure tensor and strain rate (total stress is given by $\sigma_{ij}^{\iota} + \sigma_{ij}^{\wedge}$). We present a feasibility argument for this dependence, which is shown to be thermodynamically consistent ($\sigma_{ij}^{\wedge} \&_{ij} \geq 0$). Since the anisotropic stress depends upon the structure tensor and average flaw width, we present evolution equations for these quantities. This requires us to impose constitutive closures for quantities such as $\langle r \otimes r \otimes r \otimes r \rangle$.

Coon, M. D. Maykut, G. A., Pritchard, R. S., Rothrock, D. A., and Thorndike, A. S., Modeling the pack ice as an elastic-plastic material. AIDJEX Bulletin, 24, 1-105, 1974.

Hunter, S. C., Mechanics of continuous media, Ellis Horwood, 1983.

Hibler III, W. D., A dynamic thermodynamic sea ice model, J. Phys. Oceanogr., 9, 815-846, 1979.

Fast Ice Dynamics and Anisotropic Plasticity

ROBERT S. PRITCHARD

IceCasting, Inc., 20 Wilson Court, San Rafael, CA 94901-1230
email: pritchardr@asme.org, http://www.icecasting.com, tel/fax: (415) 454-9899

My goal in participating in the SIOM workshop is to learn how fracture mechanics can improve modeling of ice behavior. As part of this learning process, I wish to review some of the processes that dominate and control ice motion. Ice fracture may describe some of these processes, but it does not describe others. Ridging is the essential process controlling ice motion. Fracture mechanics should help us to describe the initiation of ridging better, but after it begins, fracture is not a key part of the behavior. The continuation of ridging is described well by plasticity models, even down to the evolution of a single ridge.

At smaller space scales (as small as a single ridge system), an anisotropic plasticity constitutive law appears to describe the process of ridging. I will present an anisotropic elastic-plastic law (AEP) and an oriented thickness distribution that describe the changing ice conditions during ridging. I will show several simple examples of how the AEP law describes the stress and deformations.

I hope to learn how fracture mechanics can help extend our understanding of small scale ice behavior. Can it help define the tensile properties of the AEP yield surface? Its flow rule? Can it help to describe the initial formation of a ridge? Plasticity behavior is unstable if a tensile failure occurs 'instantly'. Are there ways to modify this behavior? Is there a 'slower' time scale that describes this failure? Can a decohesion law describe it? The Aidjex plasticity model accomplished much of this because the redistribution process occurred slowly. Is there a comparable description at smaller scales? Or can fracture and plasticity mechanics be melded to describe both the formation of a lead, and its evolution into a ridge? Should we develop better numerical solution schemes that explicitly describe discontinuities in solutions? I would hope to ask these questions in the workshop, and to stimulate discussions that will help improve our understanding of ice behavior.

On Simulating Oriented Failure Zones·in Sea Ice Velocity Fields

W. D. HIBLER, III, JENNIFER HUTCHINGS AND ERLAND SCHULSON

A ubiquitous feature of sea ice deformation fields is the presence of intersecting deformation patterns which change as the wind forcing changes. These fracture features form the basic characterization of sea ice deformation and account for most of the open water formation and subsequent ridging in pack ice. Investigation of anisotropic ice mechanics formulations (Hibler and Schulson, 2000) indicate that these features should form from plastic rheologies depending on the flow rule as well as the internal angle of friction. Initial basin wide simulations (Hibler,2001) with weakening, however, indicate that these features form almost as well with the appropriate isotropic rheology. Such features have not been widely reported however in most sea ice dynamics simulations to date.

To investigate the capability to model such intersecting failure patterns and to examine characteristics of these linear deformation zones, a series of idealized simulations are carried out. To examine the orientation and spacing of these features, idealized simulations where the sea ice strain and stress fields have, on the average, coincident principal axes are investigated. In these experiments the presence of random weaknesses, provided weakening due to divergence is allowed, is found to naturally allow multiple intersecting oriented features to form with the orientation in general agreement with local theory (Hibler and Schulson, 2000). The average spacing (i.e., fracture density) is found to scale with the square root of the ratio of the wind force gradient to the average ice strength in a manner independent of the water drag. An analytic theory for this dependence is developed. For a more realistic application to sea ice drift, coriolis forces and boundary layer turning angles are added so that in the absence of weaknesses the ice drift is non divergent. In this case the presence of random strengths with weakening also leads to intersecting failure features with asymmetry between the ice drift and the surface wind forcing leading to one orientation stronger than the other. The preferred orientation depends on the nature of the atmospheric pressure field. This dependence of the orientation on the pressure field characteristics (i.e., typical high or low pressure patterns) is investigated. Idealized simulations of the Arctic Basin with different wind fields together with SAR data are presented to support this result.

THEME 2: Sea-Ice Dynamics and Modeling

Scale Invariant Sea Ice Dynamics for Small Scale Sea Ice Models

W. D. HIBLER, III

While it may appear that the essential elements of ice mechanics differ at many scales a strong case can be made that this is basically an artifact of external forcing establishing scales by forming certain size regions of ice with smaller strain rates. Once this occurs than subsequent weaknesses establish the overall strength of the ice pack. However, subsequent fracturing often goes right through existing floes. In this overall presentation we examine a variety of characteristics of existing fracture based (e.g. Hibler and Schulson, 2000) sea ice models are examined. With these models finite fracture zones form (and are examined) that intersect at predictable angles which can be obtained from mathematical characteristics of the floating ice cover. These characteristics can differ from those expected under static forcing and mathematically can be developed as higher order discontinuities (velocity continuous, but higher derivatives discontinuous). Smaller scale tests of ice failure agree with this analysis and simulated results. The applicability of this type of physically based model and analysis to smaller scale problems given high enough resolution is examined based on both published and recent work.

In addition to this mechanical analysis, a number of processes relevant to ice ocean dynamics, fast ice problems and coastal currents is discussed. Recent and earlier published results, for example, on the sensitivity of a rigid fast ice formation based on plasticity and varying forcing from the ocean affected by depth and grounded ice features is examined. The overall range over which plastic flow can occur (or rigid motion with a slipping margin) is examined via a series of numerical and analytical analyses. A related problem is the effect of ice ocean coupling on coastal currents. Results showing the critical nature of including Ekman flux of sea ice (not normally included in ice ocean models, but included using the formulation of Hibler and Bryan, 1989) can significantly alter coastal circulation due to ice mechanics effects.

In addition the problem of high frequency variability, both observationally and theoretically is examined. This is a ubiquitous feature of small scale observations. Recent work on this (Heil and Hibler, in press) shows that coupling of kinematic waves in pack ice with ice mechanics is likely the main source for this phenomenon which will be increasingly important on the small scale. In addition the problem of kinematic waves in pack ice with some analytic development and available physical examples.

Modelling of Superimposed Ice Freezing and Sub-Surface Melting Based on Basis98 and Basis99 Data

BIN CHENG, JOUKO LAUNIANEN AND TIMO VIHMA
Finnish Institute of Marine Research P.O. Box 33 FIN-00931 Helsinki, Finland

INTRODUCTION
The Baltic Air-Sea-Ice Study (BASIS) project, which belongs to the GEWEX-BALTEX program, was carried out in 1998–2000. The objective of BASIS was to create and analyse an experimental data set for optimization and verification of coupled atmosphere-ice-ocean models (Launiainen, 1999). A field experiment organized in winter 1998 in the northern Baltic Sea formed the central element of BASIS. Another ice expedition was carried out in the next winter in 1999. The locations of the two field experiments were quite close to each other. Table 1 gives some basic information about the expeditions. Measurements during the BASIS-98 field experiment indicated that the ice surface was quiet variable. Snowfall was occasionally observed and snowdrift largely occurred due to frequently strong wind. On the contrary, the ice bottom showed little change indicating a thermal equilibrium stage. Observations indicated snow to ice transformation at the snow-ice interface. Numerical modelling suggested that the re-freezing of the surface melt water was a primarily source for snow-ice formation (Cheng, et al., 2001).

The BASIS-99 field experiment took place already in the early spring. During the expedition new snowfall with an average accumulation of about 9 cm was observed and surface melting was seen.

Snow present on top of the ice layer may partly transform to snow-ice. This may take place via two different physical processes: (a) flooded ocean water between snow and ice forms a slash layer and refreezes above the original ice cover; (b) melted surface and sub-surface snow water or wet snow fall and rainfall percolates down and refreezes above the original ice cover. Here, we will refer to case (b) as a superimposed ice formation.

In the Baltic Sea, the incoming snowfall was accounted on average as 25–45 mm equivalent water per month from December to February (Kolkki, 1969) and the snow ice may contribute to some 1/3 of the total ice thickness (Leppäranta and Seinä, 1982). A recent measurement made in the Gulf of Finland in winter 1998/99 indicated that even 43-55% of the total coastal land-fast ice was snow ice (Kawamura et al., 2001). The first attempt to model snow-ice formation in the Baltic Sea was made by Leppäranta (1983), while Saloranta (2000) performed a more recent modelling study of the evolution of snow-ice formation. The former one paid attention to the ice growth season. The latter one focused on the longer time-scale, i.e., the seasonal snow-ice evolution. The main mechanism for snow-ice formation in their work was (a). We study the effect of (b) on snow-ice formation. We pay attention on water through surface and sub-surface melting and its re-freezing, while the wet-snow and rainfall is not considered. The primary motivation of this work is to quantitatively understand how important is the superimposed ice formation on sea ice thermodynamics. This topic seems not to have been discussed. The model simulations are carried out with BASIS-98 and BASIS-99 field data.

The ice model presented by Launiainen and Cheng (1998) was used in this study. The model physics is resembling to those of former models (e.g. Maykut and Untersteiner, 1971; Gabison, 1987; and Ebert and Curry, 1993). But spatial attention has been given to, e.g. parameterizations of air-ice fluxes and to radiation penetration into the ice. The basic measurements for the ice modelling study were made using a weather mast (wind, temperature and relative humidity); a sonic anemometer (turbulent heat and momentum fluxes); radiometers (radiative fluxes), and an ice thermistor string (ice and snow temperatures). In addition, ice core samples were collected for ice salinity, and ice and snow thickness was manually measured every day. The weather data, solar radiation, and surface albedo were used as the external forcing for the model.

In order to study superimposed ice formation, we first need to estimate how much melting can be supplied. There are two important processes of melting:

(1) For a surface layer with its temperature larger than the melting point, the melting is calculated from the surface heat balance.

(2) The sub-surface melting happened mainly due to the effect of absorbed short-wave radiation below the surface. When the ice temperature for a sub-surface layer tends to be larger than the melting point, it is restored to the melting point, and the heat flux balance between this isothermal sub-surface layer and adjacent upper and lower snow/ice will be used for melting calculation. This procedure satisfies the continuity of conductive heat flux in snow/ice and the conservation of energy.

RESULTS AND ANALYSIS
The BASIS-98 field measurements indicated some 39% of the data with air temperature above freezing. The model run in Cheng et al, (2001) produced indeed a total surface melting of 12 cm snow. Taking into account sub-surface melting, re-run model produces about 0.5 cm (4%) more melting. The difference is actually not much. During BASIS-98, the surface melting largely occurred when air temperature was higher than the freezing point. On the other hand, downward solar radiation in February at 63°N is still quite limited and not strong enough to generate large amounts of sub-surface melting. The BASIS-99 showed only 20% data with air temperature above freezing (Table 1). However, the observed daytime average solar radiation was 35% larger than that in BASIS-98 and sub-surface melting could start. Figure 1 displays the modelled total surface snow melting. The model result indicated a total 4.5 cm melting in which about 20 % were accounted by the sub-surface melting. This simulation was analogous to that presented in Cheng et al., (2001), i.e., the external forcing was based on the weather mast measurement and the model parameters were largely based on the field measurement. Ice salinity was from 0.38 to 0.65 ppt. Freezing temperature at ice bottom was –0.2 °C. According to *in situ* measurements, the snow was

essentially divided into two layers representing the newly-fallen soft snow on top of a wind-slab hard old snow. The average snow densities are 150 kg m^{-3} and 380 kg m^{-3}, respectively. According to Sturm (1997), this suggested that the thermal conductivity were 0.056 and 0.23 Wm^{-1}K^{-1}. We further assumed the snow extinction coefficient as 25 m^{-1} and 15 m^{-1} for the upper and lower layer respectively, following Perovich (1996). The solar radiation and surface albedo were directly taken from the observations.

Some sensitivity tests were carried out in order to see the effect of snow properties on melting. For simplicity, snow is assumed as a single layer. Change of a single model parameter is made for each model test. The results are compared with the control run given in Table 2. It can be seen that the sub-surface melting is sensitive to the snow extinction coefficient while the total surface melting is sensitive to the snow thermal properties. Such conclusions support the earlier studies of increased sub-surface temperature and sub-surface melting made by Koh and Jordan (1995), who applied a high-resolution frequency-modulated continuous wave (FMCW) radar to detect the onset of sub-surface melting.

We need to emphasis that our sensitivity tests were confined to detect the effect on sub-surface melting of changing only one parameter each time. The result of such tests cannot be explained as the final truth. In reality, interaction among all parameters is expected and can enhance the effect on both melt-layer thickness and sub-surface temperatures (Bøggild et al., 1995, Liston, et al.,1999). Modelling of increased sub-surface temperature and sub-surface melting by taking into account such complex interactions among all parameters has not been made so far.

The superimposed ice is formed by refreezing of melting water. Assuming the surface melting water is totally refrozen, the modelled ice thickness is in good agreement with the field observations (Cheng et al, 2001). Such an assumption for BASIS-98 ice modelling is suitable. In that modelling, the modelled average conductive heat flux in snow was about 19 Wm^{-2} upward. If we neglect the salinity effect on latent heat of fusion, such a heat flux may generate roughly 0.6 cm frozen ice per day. In other words, the total 12.5 cm surface melting snow may take about 9 days to completely refreeze. During the melting phase, the snow surface was relatively warm and a downward heat flux in snow layer was modelled and measured indicating that a slash layer may exist for some time. On the other hand, the observed average heat flux in ice was 8.1 Wm^{-2} and upwards. This is consistent with the same direction of average heat flux in snow, which means that the slash layer between snow and ice was refrozen on a time-scale of the whole expedition.

During BASIS-99, however, the weather conditions were quite mild and not favourable for the superimposed freezing. Instead the percolated melt water may form a slash layer above original ice layer. The observed and modelled snow and ice temperature fields are given in Figure 2. Both measurement and calculation indicated quite high sub-surface temperature. Unfortunately, the uppermost thermistor recorded unreliably high snow temperature and thus is not shown here. Radiative heating of the uppermost sensors in snow or ice on clear days can lead to incorrect temperature measurement (Brandt and Warren, 1993).

Results showed that the sub-surface melting located within 10 cm below the surface. The model results clearly showed the diurnal variation of snow temperature, while measurements did not, except for the first day after deployment of the thermistor stick. This maybe due to the effect of wetness of the snow layer. The snowfall was seen occasionally mixed with rainfall since the second day of the expedition. The rainfall together with surface melt water may temporarily exist and full the porosity of the snow layer before they percolate to the snow-ice interface forming the slash layer. In addition, due to the heavy loading of snow, the saline water from the ocean may seep up to the snow-ice interface. The latent heat of the water fraction in snow can damp the daily variation of temperature of the snow layer. These effects were, however, not taken into account in the model. Further studies of those effects on superimposed ice formation are needed.

The model results of the increased sub-surface temperature effect have been difficult to verify experimentally due to the difficulties involved in measuring the temperature profile using thermal sensors embedded in snow/ice (Koh and Jordan, 1995). To verify such modelling results, more work, both theoretical consideration and field observations, is needed.

24
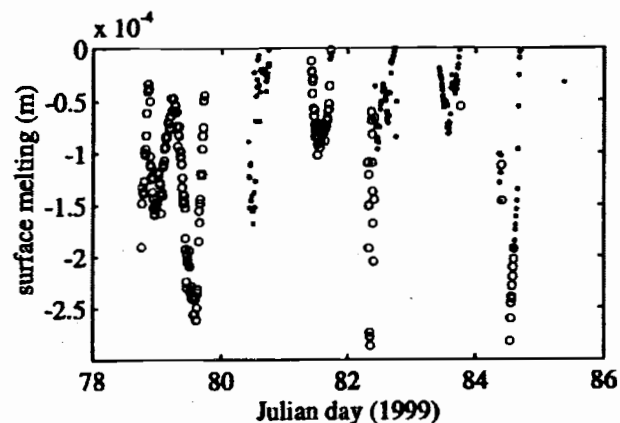
Figure 1. Modelled snow melting. The circles are surface melting while dots are calculated sub-surface melting. The melting value corresponds to a time step of 10 minutes.
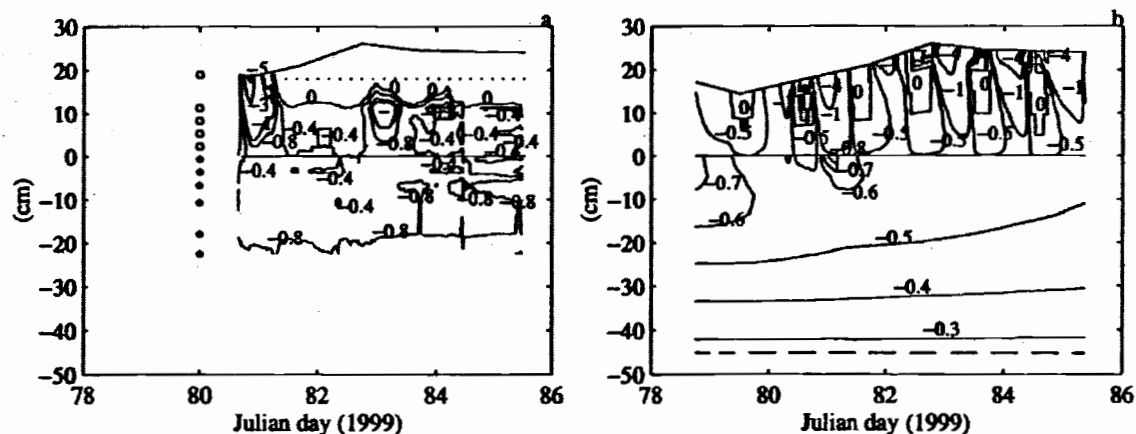
Figure 1. Snow and ice temperature (°C) during BASIS-99 experiment. a) Observed snow and ice temperature by thermistor strings. The symbols o and * give the locations of sensors in snow and ice, respectively. b) Modelled snow and ice temperature.

Table 1. The basic weather and ice information during field experiments.

	BASIS-98 (18 days)	BASIS-99 (7 days)
Time	16 Feb. – 7 March	19 Mar. – 26 March
Location	63,08.12N 21,14.67E	63,55.05N 22,56.72E
Weather conditions(average):		
wind speed V_a(10m)	7.6 ms^{-1}	4.7 ms^{-1}
air temperature T_a (10m);	–4.3 °C	–1.6 °C
relative humidity Rh (4.5m)	78 %	84 %
T_a > 0.0 °C (portion of data)	39 %	20 %
downward solar radiation Q_s		
(daytime average)	139 Wm^{-2}	188 Wm^{-2}
mean surface albedo (α_s)	0.73	0.81
Average ice thickness	38.6 cm	44.6 cm
Snow properties:		
soft snow (s)	–	9 cm
hard snow (h)	–	18 cm
average snow thickness	4.3 cm	23.1 cm
Mean water level relative to the ice surface	–1.4 cm	+7.9 cm

25

Table 2. Sensitivities of surface melting to snow properties. The melting is accounted as a decrease in the snow thickness (cm).

	κ_s (m^{-1})		ρ_s (kgm^{-3})		k_s (Wm^{-1}K^{-1})		Total melting (cm)	Sub-surface melting (cm)
	soft	dense	soft	dense	soft	dense		
Control Run (2 layers snow)	25	15	150	380	0.056	0.23	4.5	0.9 (20%)
Trail 1	25			380		0.23	3.7	0.5 (13%)
Trail 2	15			380		0.23	4.0	1.1 (28%)
Trail 3	25		150		0.056		5.3	1.3 (24%)
Trail 4	15		150		0.056		5.8	2.3 (40%)

REFERENCES

Brandt, R.E. and S.G. Warren. 1993. Solar-heating rates and temperature profiles in Antarctic snow and ice. J. Glaciol., 39(131), 99-110.

Bøggild, C.E., J.G. Winther, K. Sand and H.Elvehoy. 1995. Sub-surface melting in blue-ice fields in Dronning Maud Land, Antarctica: Observation and modelling. Ann. Glaciol., 21. 162 - 68.

Cheng, B., Launiainen, J., Vihma, T. and Uotila, J. 2001. Modelling sea ice thermodynamics in BALTEX-BASIS. Ann. of glaciology, 33: 243-247.

Ebert, E.E. and J.A. Curry. 1993. An intermediate one-dimensional thermodynamic sea ice model for investigating ice-atmosphere interaction. J. Geophys. Res. 98(C6), 10,085-10,109.

Gabison R. 1987. A thermodynamic model of the formation growth and decay of first-year sea ice. J. Glaciol. 33(113), 105-109.

Kawamura, T., Shirasawa, K., Ishikawa, N, Lindfors, A., Rasmus, K, Granskog, M.A. Ehn, J., Leppäranta, M., Martma, T. & Vaikmäe, R. 2001: Time-series observations of the structure and properties of brackish ice in the Gulf of Finland. Ann. of Glaciol. 33: 1-4.

Koh, G., and R. Jordan. 1995. Sub-surface melting in a seasonal snow cover. J. Glaciol., 41(139), 474-482.

Kolkki, 1969: A review on the climate in Finalnd (in Finnish). Ilmat. Lait. Tied. 18.

Launiainen, J., ed. 1999. BALTEX-BASIS Data Report 1998. Geesthacht, Germany. International BALTEX secretariat. (Publication14).

Launiainen, J. and B. Cheng. 1998. Modelling of ice thermodynamics in natural water bodies. Cold Reg. Sci. Technol., 27(3), 153-178.

Leppäramta, M. & Seinä A. 1982: Statistics of fast ice thickness along the Finnish coast, - Finnish Mar. Res. 249: 62-71.

Leppäranta, M. 1983: A growth model for black ice, snow ice and snow thickness in subarctic basins. - Nordic Hydrol. 14: 59-70.

Liston, G.E., J.G. Winther, O. Bruland, H. Elvehoy and K. Sand. 1999. Below-surface ice melt on the coastal Antarctic ice sheet. J. Glaciol., 45(150), 273-285.

Maykut, G.A. and N. Untersteiner. 1971: Some results from a time dependent thermodynamic model of sea ice. J. Geophys. Res., 76(6). 1550-1575.

Perovich, D.K. 1996. The optical properties of sea ice. CRREL Rep. 96-1.

Saloranta, T. 2000: Modelling the evolution of snow, snow ice and ice in the Baltic Sea, - Tellus 52A: 93-108.

Sturm, M., J. Holmgren, M. König and K. Morris. 1997. The thermal conductivity of seasonal snow. J. Glacoil., 43(143) 26-40.

Modelling Observed Sea Ice Deformation in the Western Arctic

JENNIFER HUTCHINGS AND WILLIAM D. HIBLER III

Sea ice deformation may be characterised by narrow zones of failure between rigid aggregates of ice. SAR RGPS observations of deformation [Personal Communication: Kwok \& ASF] show these faults extend hundreds of kilometres across the Arctic ice pack. Failure zones are typically regions of lead opening or ridge building. Correctly modelling these processes will improve estimates of sea ice mass balance and open water fraction. Deformation features may be modelled with an isotropic rheology and weakening, if the spatial distribution of ice strength is randomly varying. We believe failure occurs along characteristic directions, which depend upon the local confinement ratio between principle stress components, boundary conditions, the shape of yield curve and flow rule relating stress to strain rate [Hibler & Schulson 2000].

Quantitative comparisons are made between modelled ice deformation in the western Arctic and RGPS failure zones. The statistical distribution of fracture density (total length of fractures per unit area) and orientation is estimated from RGPS deformation data and compared to model results. Current isotropic non-linear rheological models (ellipse [Hibler 1979], sine lens, mohr-coulomb [Ip 1993] and modified coulombic [Hibler & Schulson 2000]) are validated against this data. The criteria for choosing a plastic model for sea ice at the 10 km scale are revisited, and model investigations are made to understand what controls the direction and orientation of failure zones in the Beaufort Sea.

An Impact of Sub-Grid-Scale Ice-Ocean Dynamics on Sea-Ice Cover

DAVID M. HOLLAND AND PETTERI UOTILA

A coupled sea-ice–ocean numerical model is used to study the impact of an ill-resolved sub-grid-scale sea-ice–ocean dynamical process on the areal coverage of the sea-ice field. The process of interest is the transmission of stress from the ocean into the sea-ice cover and its subsequent interaction with the sea-ice internal stress field. An idealized experiment is performed to highlight the difference in evolution of the sea-ice cover in the circumstance of a relatively coarse-resolution grid versus that of a fine-resolution one. The experiment shows that the ubiquitous presence of instabilities in the near-surface ocean flow field as seen on a fine-resolution grid. effectively leads to a sink of sea-ice areal coverage that does not occur when such flow instabilities are absent, as on a coarse-resolution grid. This result also implies that a fine-resolution grid may have a more efficient atmosphere–sea-ice–ocean thermodynamic exchange than a coarse one. This sink of sea-ice areal coverage arises because the sea-ice undergoes sporadic, irreversible plastic failure on a fine-resolution grid that, by contrast, does not occur on a coarse-resolution grid.

Applications of a Marginal Ice Zone Model

LEIF TOUDAL
Technical University of Denmark

An ice and salt flux analysis model for the marginal ice zone has been developed. It is forced by daily average winds and daily satellite ice observations. The measure of producing ice in the model is obtained from a comparison between the advected ice field from the previous time step and the actual satellite ice observations. The model has been applied to the Greenland Sea, the Bering Sea and the Beaufort and Chukchi Seas. Results of model now-casts will be presented and discussed.

On the Formation and Orientation of Leads and Ice Ridges in the Frame of Anisotropic Deformation

KEGUANG WANG

Department of Physical Sciences, University of Helsinki, Helsinki, Finland
National Research Center for Marine Environment Forecasts, Beijing, China

Leads and ice ridges are two permanent guests in the polar oceans, which are of great importance to the polar ocean air–sea heat exchange, and in turn the global climate. In order to better describe and interpret them, recently quite many efforts have been made upon the anisotropic failure models (e.g. Coon et al., 1992, 1998; Hibler and Schulson, 1997, 2000). However, Hibler (2001) found the isotropic models can also obtain the similar deformation field as the anisotropic models.

In this paper, other than the consideration from the failure models, an anisotropic deformation theory is employed to describe the formation and orientation of the leads and ice ridges. The main ideas of the theory are as follows. (1) The deformation of pack ice is partially anisotropic, which means only part of. the maximum shear strain rate contributes to the anisotropy of the deformation. A parameter k, the index of the anisotropic deformation of pack ice, is introduced to express the partial anisotropy. (2) The actual principal strain rates can be regarded as independent and orthogonal, which means that the deformation corresponding to the principal orientations can be treated separately. That is, the general divergence is equivalent to the two independent extending, the general convergence is equivalent to two independent contracting, and the general shear is equivalent to one contracting and one extending.

The study shows that the formation and orientation can be expressed by the anisotropic deformation even with an isotropic constitutive law. And we find that the formation of open water can be expressed explicitly, while that of ice ridges is a subgrid process, which needs parameterization. The results are compared against the parameterization schemes proposed by Thorndike et al. (1975) and Hibler (1980) and discussed by Martinson et al. (1995). The formation and orientation of the curvilinear patterns are deduced, compared with the discussions of Pritchard (1988) and Erlingsson (1988). In addition to deduce the frictional angle and the types of characteristics, this paper tries to state the real orientation of these curilinear patters, provided that the deformation field is known.

Mechanical Simulation of Shore Fast Ice Break-Up: Kara And Laptev Seas

D. ZYRYANOV[1], D. DIVINE[1], AND R. KORSNES[2]

[1]*Norsk Polarinstitutt, Troms", Hjalmar Johansensgate 14, Norway; email: denis.zyryanov@npolar.no*
[2]*Norwegian Defense Research Establishment (FFI), Division of Electronics, Post Box 25, NO-2027, Kjeller, Norway; email: reinert.kornes@ffi.no*

The mechanical stresses caused by wind and ocean currents play an important role in ice cover break up. In our work we focus on the fast (attached to a shore) ice development in the Kara and Laptev Sea basins. During winter, these areas are partly covered by ice, whose destruction and development is subjected to strong offshore winds. The geomechanical model applied in the work is based on the Particle Flow Code (PFC) that is widely being used recently in numerous mechanic applications. The PFC deals with circular particles-disks, which can be bonded together to simulate rigid bodies and continuous media. At the start of the modeling the disks fill all the free space in the model domain. Then an external load is applied, simulating wind drag force. It leads to the mechanical break up of the ice sheet and causes ice drift. The simulation results revealed areas sensitive to the wind stress fluctuations and sea ice physical properties—areas of local mechanical instability. One such area was discovered in vicinity of Sverdrup island in the Kara Sea basin. Finally, we compare the simulation results with in-situ observations (AARI dataset) of the fast ice in the Kara and Laptev seas. The results demonstrate a coincidence of the areas of mechanical instability with observed annual variations in fast ice edge, confirming that shore geometry play a significant role in ice cover spreading and ultimately defines its outline and development.

THEME 3: Small-Scale and Basin-Scale Coupled Ice–Ocean Modeling

Parameterization of Thin Ice in a Coupled Ice–Ocean Model: Application to the Seasonal Ice Cover in the Sea of Okhotsk

M. IKEDA[1,2], H. SHINKAI[1,3] AND T. WATANABE[4]

[1]Graduate School of Environmental Earth Science, Hokkaido University
[2]also at Frontier Research System for Global Change
[3]presently at Applied Technology Institute
[4]Japan Sea National Fisheries Research Institute, Fisheries Agency

The Okhotsk Sea is partially covered by sea ice from November to May and an indicator of climate variability. A coupled ice-ocean model has been implemented to predict the sea ice cover and also to explore individual processes important to the ice cover. A new component added to the original two-category ice model is a very thin ice category, which would be otherwise open water or mixture of open water and thick ice. The thin ice can be crucial to ice formation by reducing atmospheric cooling and to ice reduction by reflecting solar radiation. This ice category is assumed to merge with the thick ice category as it is compressed as consequence of ice internal pressure. The model simulation has shown that both effects of reducing atmospheric cooling and reflecting solar radiation give minor differences in the total ice volume at least in the simulated cases. However, the ice concentration increases and is better simulated in the new version, comparable with satellite remote sensing data.

Sea Ice Modelling for the Bohai Sea of China

YU LIU, HAI LI, JIE SU, SHAN BAI, QINZHENG LIU, HUIDING WU

The ice in the Bohai Sea is first-year ice and relatively thin. Temporal variation of ice conditions is very complex in the Bohai Sea. Exploratory drilling and planning for production and transportation for oil and gas in the Bohai Sea during winter have raised great demand for numerical forecast of sea ice. A dynamic-thermodynamic ice model with three levels (level ice, rubble and open water) for simulating the ice growth, decay and drift in the Bohai Sea is developed on the basis of a review of the climate and ice conditions in the Bohai Sea and the earlier sea ice modeling studies. The routine satellite remote sensing data opened up possibilities for operational numerical sea ice forecast. The output of T106L19 atmospheric model from National Meteorological Center of China was used for the operational numerical ice prediction of the Bohai Sea and the northern Yellow Sea.

The ice model was coupled with Blumberg's ECOM-si model, a three-dimension, primary equation and semi-implicit ocean model, for studying the ice-sea interaction of the shallow water and modelling the variation of ice conditions of the Bohai Sea. It is showed from simulation that oceanic effects on ice are important, especially, the tide driven effect is more important in the Bohai Sea. Therefore, the effect of tidal current must be considered in forecasting the local sea ice of the Bohai Sea. And as a result of the joint effects of wind and tidal current, the pile-up of sea ice is greater than that affected by wind stress only. The coupled model considers the dynamic and thermodynamic effects at the interface of sea/ice, sea/air and ice/air. The ocean heat flux is a very important factor for the simulation of growth and decay of ice. An empirical formula is used to calculate the ocean heat flux in the Bohai Sea. The two cases of ice growth and decay processes are hindcasted and the results are satisfied.

The ice model is also coupled with the Princeton Ocean Model (POM) to study the relation of ice cover variation with the heat budget at the interface of ice/sea, air/ice and air/sea in the Bohai Sea during the ice growth period. The case studies show that the thermodynamic effects from atmosphere and ocean are very important to the Bohai Sea ice, especially during the period of freeze-up, when the ice edge can often extend tens of miles in several days. Cloud is a sensible element to the heat budget at the surface of ice and water.

A multi-category particle-in-cell sea ice model was applied in the Bohai Sea. Ice data acquisition in the Bohai Sea is mainly from conventional observation at coastal stations, ship survey, aircraft reconnaissance and satellite remote sensing imagery, but the amount of data is far from sufficient. Using the ice data of the Arctic and Baltic Sea, we start preliminary research of sea ice morphology and explore the relationship between ice thickness distribution and the environmental meteorologic and oceanic elements. The objective is to put forward adequate ice thickness distribution function of the Bohai Sea. At the same time, a series of numerical experiments of PIC model under the ideal meteorologic and oceanic forcing fields were done. On the basis of above studies, a multi-category thickness distribution ice model in the Bohai Sea is developed. The model enhances the resolution and can simulate the dynamic process of sea ice in more detail. The digitalization and application of Modis remote sensing images of sea ice provide ice thickness and concentration distribution in higher resolution, which can offer ice thickness distribution of all the particles in one cell. All these make it possible to simulate ice drift, strength and thickness for a single point (such as drilling platform).

A Nested Coupled Ice–Ocean Model for the Beaufort Sea

JIA WANG, QINZHENG LIU, MEIBING JIN
International Arctic Research Center-Frontier Research System for Global, Change, University of Alaska Fairbanks, Fairbanks, AK 99775-7335; email: jwang@iarc.uaf.edu
Institute of Marine Science/SFOS, University of Alaska Fairbanks, Fairbanks, Alaska 99775-7225

A nested coupled ice-ocean model is being developed under the CMI/MMS project entitled A Nowcast/Forecast Model for the Beaufort Sea Ice-Ocean-Oil Spill System (NFM-BSIOS). At the first step, the nested ocean model (3.4 km) is described. We developed a transport-conserved nested scheme to pass information from the coarse (27.5 km) model to the fine model. The fine (-resolution) ocean model was run for a seasonal cycle, far beyond the need for the operational purpose (Wang, 2001). We found that the surface circulation follows the wind direction (to the west), while the slope current along the Beaufort Sea slope is reproduced below 100 m, flowing to the east, just opposite to the surface current. There are some mesoscale eddies in the fine model. Neither the slope current nor the mesoscale eddies are captured in the coarse model. Thus, this fine nested model preliminarily captures some dynamical features in the Beaufort Sea and its shelves.

Furthermore, upwelling along in the Beaufort Sea in winter can be detected due to the strong Beaufort High-driven anticyclonic circulation, which produces an offshore Ekman drift and favors a upwelling of the Atlantic Water in the lower layer. As a result, sea ice thickness and concentration near the coast reduce due to the warming of the Atlantic Water.

Thermodynamics Critical to Arctic Mixed Layer Systems

ROLAND WILLIAM GARWOOD, JR.
Naval Postgraduate School, Department of Oceanography, Monterey, CA 93943
email: garwood@nps.navy.mil

The thermodynamics of seawater at near-freezing temperatures is critical for modeling mixed layer entrainment of heat that determines ice thickness, polynya formation, and the location of MIZs. This thermodynamics is related to nonlinearities in the equation of state for seawater, which are greatly augmented wherever the sea surface temperature approaches freezing. Particularly important is "thermobaricity", the dependence of thermal expansion α on temperature and pressure. This phenomenon is not resolved in coarse-grid hydrostatic models, but considerable insight has been provided by high-resolution nonhydrostatic large-eddy simulation (LES), which resolves turbulence, internal waves,

dispersion, convection and fine-scale transport. Phenomena that need to be addressed in regional arctic models include four enumerated below and depicted in the schematic figure:

1. Mixed-Layer turbulent kinetic energy (TKE) may be increased several-fold by the thermobaric amplification of the buoyancy flux. Commonly used parameterizations of ocean mixing do not yet include this physics.

2. Although buoyancy is well conserved in vertical advection of temperate water masses, it is not conserved in the polar seas coastal and deep-water subduction. This is a severe limitation for layered models that presume a constant potential density for each layer.

3. "Thermobaric stability" is an increase in the hydrostatic stability of seawater having positive spiciness ($\alpha\delta T+\beta\delta S>0$) and nearly density-compensating T-S structure, $\alpha\delta T-\beta\delta S \approx 0$. This causes spicy warmer ($\delta T>0$) and saltier ($\delta S>0$) parcels to resist vertical mixing because of this newly recognized thermobaric component to the buoyancy frequency, $N_{rg}^2=\alpha_o g\delta T/H_\alpha$, where total buoyancy frequency is $N^2=\partial b/\partial z+N_{rg}^2$. This added component depends upon the thermobaric depth H_α. This phenomenon enables internal gravity waves to exist without any vertical buoyancy gradient, and it helps explain lateral intrusion of filaments of spicy water across T-S frontal zones. Furthermore, the theory predicts reduced stability for cold and fresh filaments with negative spiciness. This process is potentially important in enhancing shoreward transport but reducing the flux of suspended and dissolved material from the shelf into the Arctic Ocean interior.

4. A critical depth h_{cr}† for maintenance of open water and polynyas under freezing atmospheric temperatures is predicted because of thermobaricity. Whenever the mixed layer depth exceeds this depth, the entrainment heat flux Q_e will exceed the surface heat loss to the atmosphere (Q_o), resulting in ice melting regardless of the rate of heat loss to the atmosphere from the ice-mixed layer system. This is a positive feedback mechanism for warming the surface layer, limiting ice formation, and cooling the ocean interior. It undoubtedly plays a role in establishing the extent and geographic evolution of the marginal ice zone, and in the maintenance of polynyas and their entrainment of nutrient-rich water into the surface layer.
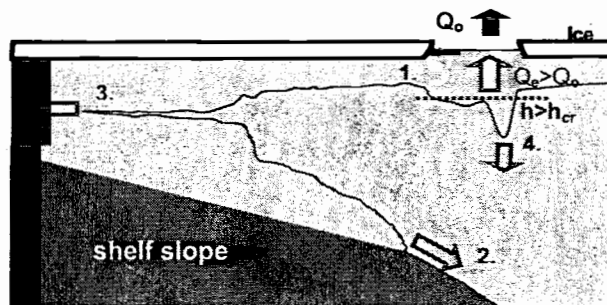
Figure 1. Thermobaric process important to the coupled air-sea-ice system.

A Numerical Investigation of Sea Ice Dynamics in the Gulf of Riga

KEGUANG WANG[1], MATTI LEPPÄRANTA[1] AND TARMO KÕUTS[2]
Department of Physical Sciences, University of Helsinki, Helsinki, Finland
Department of Marine Physics, Estonia Marine Institute, Tallinn, Estonia

The Gulf of Riga is a rather small semi-enclosed water body in the eastern part of the Baltic Sea bordering on Estonia and Latvia. It only covers ~16400 km² with a volume of ~240 km³ and a quite square shape. In normal and severe winters, the gulf is often covered by ice, while in mild winters it is often ice-free. Based on the ice charts from the Finnish Institute of Marine Research, the ice cover in the gulf shows the following

characters. (1) The coastal fast ice zone remains similar in different normal and severe winters. That is, the demarcation of the fast ice and drift ice is basically controlled by the topography of the gulf (Wang et. al., 2001). (2) When ice thickness is about 20–40 cm (estimation), there are only cases of drift ice deforming mildly while forced against the coast even in the condition of wind speed of 15 m/s, this is, however, pretty different with the ideal experiment which yields clearly high ice piles along the coast (Wang & Leppäranta, 2001), in which the parameters are all the same as those used for the whole Baltic sea (Zhang, 2000).

In order to investigate the sea ice scale problem and verify the capability of the dynamics sea ice model running in small-scale conditions, a field experiment will be carried out in late March 2002. This paper will thus conclude the experiment results, study the scale problem and propose a group of appropriate parameters for the sea ice model.

Modelling the Formation and Circulation Processes of Water Masses and Sea Ice in the Gulf of St. Lawrence, Canada

FRANÇOIS J. SAUCIER AND FRANÇOIS ROY
Ocean Sciences Branch, Fisheries and Oceans, Maurice Lamontagne Institute, Mont-Joli, QC G5H 3Z4, Canada; email: saucierf@dfo-mpo.gc.ca

The seasonal cycle of water masses and sea ice in the Gulf of St. Lawrence is examined using a 5 km resolution three-dimensional coastal ice-ocean model with realistic tidal, atmospheric, hydrologic, and oceanic forcing. The model includes a level 2.5 turbulent kinetic energy equation. A model simulation over 1997-98 is verified against available data on sea ice, temperature, and salinity. The results demonstrate a consistent seasonal cycle in atmosphere-ocean exchanges and the formation and circulation of water masses and sea ice. The accuracy of radiative, momentum and sensible heat exchanges at the sea surface, and the production of turbulent kinetic energy from winds and tides, are critical to the accuracy of the modeled circulation. The sea ice thickness and concentration are highly dependent upon stratification and the fall and winter mixing through the upper 100 m of the water column. Sensitivity analyses show that only few storms during late December and early January can trigger highly different responses in sea ice production over the following months. Finally, we examine the sea ice cover variability over synoptic to seasonal time scales when comparing the use of an elastic-viscous-plastic rheology (e.g., Hunke and Ducowicz, 1997), a simpler cavitating fluid rheology (e.g., Flato, 1994), and ARGOS and Radarsat-derived sea ice dynamics.

Flato, G. M., & W. D. Hibler, Modeling pack ice as a cavitating fluid, J. Phys. Oceanogr., 22, 626-650, 1992.
Hunke, E. C., & J. K. Dukowicz, An elastic-viscous-plastic model for sea ice dynamics. J. Phys. Oceano., 27, 1849-1867, 1997.
Sauçier, F. J., F. Roy, D. Gilbert, P. Pellerin, & H. Ritchie, The formation and circulation processes of water masses in the Gulf of St. Lawrence. J. Geophys. Res., in press.

Coordinated Changes of Sea-ice and Ocean Properties in the Beaufort and Chukchi Seas

XIANGDONG ZHANG AND MOTO IKEDA
Frontier Research System for Climate Change/International Arctic Research Center, University of Alaska Fairbanks, AK99775, USA; email: xdz@iarc.uaf.edu

During recent decades, dramatic changes have been observed in the Arctic atmosphere, sea-ice and ocean. For example, the sea level pressure shows unprecedented persistent and low values; ocean part

exhibits a 1-degree warmer Atlantic layer in the Canadian Basin; sea-ice concentration decreases at the rate of about 3% and sea-ice thickness drops about 40% at some sites. All of these have been manifested in the Beaufort and Chukchi Seas. To explore these changes and their associated underlying physical processes, we employed a coupled Arctic sea-ice/ocean model and carried out modeling experiments forced by the NCEP/NCAR reanalysis data. Results show that the model captures the changes of sea-ice and ocean properties obtained in observations. The phase shift of atmospheric leading mode, Arctic Oscillation (AO), is a major factor responsible for such changes. Corresponding to positive AO phase, anomalous higher air temperature and windstress ranges from the Chukchi Sea to the Beaufort Sea. In the negative AO phase, the signs of anomalous air temperature and windstress are reversed. Coordinated changes of sea-ice and ocean properties in both shelf seas have been detected, which is characterized by thinning of sea-ice and salinity increasing of upper ocean in the Chukchi Sea while thickening of sea-ice and freshening of upper ocean in the Beaufort Sea. They are governed by thermodynamic and dynamic interactions.

Modeling the Arctic Ocean and Its Sea Ice: From a Local to Basin Scale

WIESLAW MASLOWSKI
Department of Oceanography, Naval Postgraduate School, Monterey, CA 93943, USA
email: maslowsk@nps.navy.mil

As a part of an effort by the Office of Naval Research to upgrade the Navy operational Polar Ice Prediction System (PIPS) model, a new model version named PIPS 3.0 has been developed and initially tested at the Naval Postgraduate School in collaboration with several academic institutions. The main emphasis of this work was on improvements in sea ice leading to better prediction of open water regions, i.e. leads and polynyas within the ice pack. Ability to predict such narrow (of order O(10km)) and long (of order O(1000km)) features in the sea ice is of interest and importance to the US Navy submarine operations.

One of the requirements to advance PIPS predictive skill involved increasing model horizontal grid cell resolution. The PIPS 3.0 grid was configured at ~9 km and 45 levels using the rotated coordinate system to eliminate singularity problem at the North Pole. The model domain extends from the North Pacific (~30°N), over the Arctic Ocean, the Canadian Archipelago and the Nordic Seas, to the North Atlantic (to ~45°N). This approach allows accounting for all the northern latitude ice covered regions at a high and nearly uniform resolution. This research is an extension of our previous modeling work (e.g. Maslowski et al., 2000, Maslowski et al., 2001).

Model improvements have been so far tested in two steps. The first test was designed to examine the effects of higher resolution on the existing ice model coupled to an ocean model with more realistic bathymetry. A 60-year integration of the coupled ice-ocean model has been completed. This model run has been forced with daily-averaged realistic atmospheric fields from the European Centre for Medium-range Weather Forecasts (ECMWF) 1979–1993 reanalysis. The coupled model adapts the Los Alamos National Laboratory (LANL) Parallel Ocean Program (POP) ocean model with a free surface. The sea ice model uses a viscous-plastic rheology, the zero-layer approximation of heat conduction through ice and a simplified surface energy budget. Many improvements, such as the ice edge position in the Nordic and Bering/Chukchi Seas, are results of more realistic modeling of the upper ocean currents and hydrography. More results from this experiment are available at <www.oc.nps.navy.mil/~pips3>.

The second test has focused on evaluating the new sea ice model ability to predict leads and polynyas. A 20-year integration of the stand-alone 9-km sea ice model with a mixed ocean layer has been completed. This model uses the most recent version of sea ice model (CICE 3.0) developed at LANL. It contains an improved calculation of ice growth/decay based on work of Bitz and Lipscomb (1999). It has been configured to use five sea ice categories with 4 layers per category, a snow layer in each category, the EVP rheology (Hunke and Dukowicz, 1997), the remapping of sea ice transport (Lipscomb and Hunke, 2002) and ice thickness (Lipscomb, 2001). The realistic daily-averaged 1979–1988 ECMWF atmospheric data has been used to force the model. Mostly output from this second test will be discussed. Results on model representation of leads and polynyas over the Chukchi/Beaufort Sea region will be presented,

including sea ice concentration, drift, divergence, shear, and vorticity. Further model evaluations are planned as results from integration of the new sea ice model coupled to the pan-Arctic ocean model become available.

Bitz, C. M., and W. H. Lipscomb, 1999: An energy conserving thermodynamic model of sea ice. J. Geophys. Res., 104(C7), 15669-15677.

Hunke, E.C., and J.K. Dukowicz, 1997: An elastic-viscous-plastic model for sea ice dynamics. J. Phys. Oceanogr., 27:1849-1867.

Lipscomb. W.H., 2001: Remapping the thickness distribution in sea ice models. J. Geophys. Res., 106:13,989-14,000.

Lipscomb, W. H., and E. C. Hunke, 2002: Modeling sea ice transport using incremental remapping. Mon. Wea. Rev., submitted.

Maslowski, W., B. Newton, P. Schlosser, A. Semtner, and D. Martinson, 2000: Modeling recent climate variability in the Arctic Ocean. Geophys. Res. Lett., 27(22), 3743-3746.

Maslowski, W., D. C. Marble, W. Walczowski, and A. Semtner, 2001: On the large scale shifts in Arctic Ocean and sea-ice conditions during 1979-98. Annals of Glaciology, 33, 545-550.

A Coupled Ice-Ocean Model in the Pan Arctic and North Atlantic Ocean: Seasonal Cycle

MEIBING JIN AND JIA WANG

Institute of Marine Institute and International Arctic Research Center-FRSGC
University of Alaska Fairbanks, Fairbanks, AK 99775 USA; email: jwang@iarc.uaf.edu

A coupled ice-ocean model (CIOM) was applied to investigate the general circulation of the pan Arctic and North Atlantic Ocean (PANAO). The annual mean was computed under daily wind and other atmospheric forcings using the NCEP/NCAR reanalysis, restored to the surface monthly climatological temperature and salinity. The simulated total transport of the Labrador Sea is consistent with historical observation. The western North Atlantic is dominated by the cyclonic Labrador Current system, while the eastern North Atlantic is dominated by the anticyclonic gyres. Greenland Basin and Noweigian Basin both have a cyclonic gyre.

In Fram Strait, the model simulated an outflow of Arctic surface water from the Greenland side and inflow of the North Atlantic Water from the eastern side. The simulated temperature and salinity in Fram Strait indicate the intrusion of the Atlantic Water and the outflow of the Arctic surface water. In the Arctic Basin, the simulated total transport is cyclonic in both the Eurasian Basin and the Canadian Basin although the surface ocean current is anticyclonic.

The observed sea ice concentration, thickness, heat flux, and freshwater thickness are used to validate the model simulations. The consistency and difference are discussed.

The Impact of Numerical Resolution on Predictions of a Thermodynamic Sea Ice Model

BIN CHENG

Finnish Institute of Marine Research, P.O. Box 33 FIN-00931, Helsinki

INTRODUCTION

The numerical integration of the heat conduction equation is one of the main components of ice thermodynamic models. The spatial resolution the in ice normally varies from a minimum of three layers up to a few tens of layers. The temporal resolution varies from a few minutes up to hours. In the case of process studies, fine resolution models are usually applied, in order to obtain details. A prototype of such a model was developed by Maykut and Untersteiner (1971). For climate studies, coarse resolution models are often used, in order to enable faster long-time simulations. A typical example is the model of Semtner (1976).

Physically, the thermal variation of sea ice is a complex process. The interfacial surface fluxes between the ice and the atmosphere and the in-ice heat conduction are strongly affected by the ice thickness (Maykut, 1978). The in-ice thermal regime responds to the heat flux balance at its surface and bottom. Its multi-phase constituency (ice crystal, solid and liquid brine, inclusion of air and other impurities) varies concurrently with the changes in heat flow and energy storage inside the ice. One has to define a thin interfacial layer (surface layer) with a finite mass and heat capacity to study the surface heat balance, especially for a fine resolution model. The ice mass and heat storage clearly depend on the thickness of the surface layer, and this dependence, in general, is non-linear because the brine pockets and vapour bubbles affect the physical and thermal properties of the ice. The solar radiation flux, which penetrates into the interior of the ice or snow, is strongly attenuated in the surface layer. The surface heat balance therefore tends to be established differently depending on the various assumptions made for the model spatial resolution. Below the surface, the absorbed solar radiation is an internal heat source and plays an important role in the heat conduction of the upper ice layer. The estimation of this term using a finite difference scheme is directly affected by the spatial resolution used. To systematically demonstrate how spatial resolution affects model results is one of our motivations for this study.

THEORETICAL BACKGROUND

The sea ice model

The ice model presented by Launiainen and Cheng (1998) is used in this study. The basic model equations read:

$$(\rho c)_{i,s} \frac{\partial T_{i,s}(z,t)}{\partial t} = \frac{\partial}{\partial z}\left(k_{i,s} \frac{\partial T_{i,s}(z,t)}{\partial z}\right) - \frac{\partial q_{i,s}(z,t)}{\partial z} \tag{1}$$

$$(1-\alpha_{i,s})Q_s - I_0 + Q_d - Q_b(T_{sfc}) + Q_h(T_{sfc}) + Q_{le}(T_{sfc}) + F_c(T_{sfc}) - F_m = \Gamma(T_{sfc}) = 0 \tag{2}$$

$$T_{bot} = T_f \tag{3a}$$

$$-\rho_i L_f \, dH_i/dt = -(k_i \, \partial T_i/\partial z)_{bot} + F_w \tag{3b}$$

The ice temperature is governed by the heat conduction equation (1), while Eq. (2) and (3) represent the boundary conditions for the temperature, and the heat and mass balance at the surface and bottom.

In Eq. (1) T is the temperature, ρ is density, c is specific heat, k is thermal conductivity, q(z,t) is the amount of solar radiation penetrating below the surface, t is time, and z is the vertical coordinate below the surface (positive downwards). Subscripts i and s denote ice and snow, respectively. The thermal conductivity and heat capacity of sea ice are given as: $k_i = k_{i0} + \beta s_i/(T_i - 273.15)$ and $(\rho c)_i = \rho_0 c_0 + \gamma s_i/(T_i - 273.15)^2$, following Maykut and Untersteiner (1971), where k_{i0}, ρ_0 and c_0 are the thermal conductivity, the density and the specific heat of pure ice, respectively, and s_i is the ice salinity, β and γ are constants.

In Eq. (2) α is the surface albedo. The downward short-wave radiation (Q_s) is calculated by an empirical formula (Shine, 1984) with the cloudiness factor (C) of Bennett (1982):
$Q_s = S_0\cos^2 Z/[(\cos Z+1.0)\ e\ 10^{-3}+1.2\cos Z+0.0455](1-0.52C)$ where S_0 is the solar constant, Z is the local solar zenith angle, e is the vapour pressure and C is from 0 to 1.

The solar radiation penetrating below the surface (I_0) is that part of the energy that contributes to internal heating of the ice/snow. It is the portion of solar radiation that does not contribute directly or immediately to changes in mass or temperature at the surface.

The incoming atmospheric long-wave radiation (Q_d) is calculated by the formula of Efimova (1961) with the cloud effect according to Jacobs (1978): $Q_d = (0.746+0.0066e)\sigma T_a^4(1+0.26C)$ where σ is the Stefan-Boltzmann constant and T_a is the air temperature. The outgoing long-wave radiation from the surface is estimated by the Stefan-Boltzmann law $Q_b = \varepsilon\sigma T_{sfc}^4$ with a constant surface emissivity ($\varepsilon = 0.97$), where T_{sfc} is the surface temperature.

The turbulent sensible heat (Q_h) and latent heat (Q_{le}) fluxes are calculated by the bulk formulae:
$Q_h = -\rho_a c_p C_H(T_{sfc}-T_{za})V_{za}$ and $Q_{le} = -\rho_a L_v C_E(q_{sfc}-q_{za})V_{za}$, where ρ_a is the air density, c_p is the specific heat of air, L_v is the enthalpy of vaporization, C_H and C_E are the turbulent transfer coefficients, V is wind speed, q is the specific humidity, and the subscripts sfc and za refer to the surface and a height of za in the air, respectively. The coefficients C_H and C_E are estimated using the Monin–Obukhov similarity theory with stability effects based on Högström (1988) in unstable cases and Holtslag and de Bruin (1988) in stable cases. An aerodynamic roughness value of 0.001 m is used and the thermal roughness length is calculated according to Andreas (1987).

The surface conductive heat flux is F_c and the heat flux due to surface melting is F_m. When T_{sfc} tends to be larger than the freezing temperature(T_f), T_{sfc} remains as T_f, the heat used for melting is $F_m = \rho_{i,s}\cdot L_f\cdot dH_{i,s}/dt$, where L_f is the latent heat of fusion assumed to be constant, and $H_{i,s}$ is the thickness of ice or snow. We should emphasise that Eq. (2) is actually a Neumann type flux boundary. It is a complex polynomial of the surface temperature. Therefore, instead of directly applying it in numerical sea ice modelling, T_{sfc} is usually solved iteratively from Eq. (2) and used as the upper boundary (Dirichlet type) for the numerical scheme of Eq. (1) (e.g., Maykut and Unsersteiner, 1971, Gabison, 1987, Ebert and Curry, 1993, Launiainen and Cheng, 1998).

In Eqs. (3a) and (3b) the ice bottom temperature (T_{bot}) is constrained to be the freezing temperature and F_w is the oceanic heat flux, assumed constant.

An implicit 6-point symmetrical CN scheme, which was derived on the basis of the numerical integral interpolation method (Cheng, 1996), is used to solve the heat conduction equation. The scheme derived by this method has been mathematically proven to be conservative (Li and Feng, 1980). The model parameters are listed in Table 1. The sea ice properties are based on average values from the literature and field measurements in the Baltic Sea.

Penetrating solar radiation in ice and snow
The solar radiation penetrating into sea ice depends strongly on the wavelength of the irradiance, on its angle of incidence, on the structure of the sea ice and on sky conditions. For ice modelling purposes, however, simple parameterizations based on the Bouguer-Lambert law are often used (e.g., Untersteiner, 1964, Maykut and Untersteiner, 1971, Grenfell and Maykut, 1977). In these studies
$q_i(z,t) = i_0\cdot(1-\alpha_i)Q_s\ e^{-\kappa i(z-zi)}$, z > zi, is described as an exponential decay through the ice depth, where $i_0 = F(C, Ci)$ is defined as the fraction of the wavelength-integrated incident irradiance transmitted through the top zi = 0.1 m of the ice, and parameterized according to the sky conditions (C) and sea ice colour (Ci), for example, $i_0 = 0.18(1-C) + 0.35C$ for white ice, and $i_0 = 0.43(1-C) + 0.63C$ for blue ice (Grenfell and Maykut, 1977; Perovich, 1996), and κi is the bulk extinction coefficient below zi varying from 1.1 to 1.5m^{-1} (Untersteiner, 1961). Near the surface, κi can be one or two orders of magnitude larger than 1.5 m^{-1} (Grenfell and Maykut, 1977). Accordingly, a two-layer parameterization scheme for $q_i(z,t)$ is assumed in our ice model. In the top 0.1 m of the ice, we applied $q_i(z,t) = (1-\alpha_i)Q_s\ e^{-\kappa 1z}$, 0 < z < zi. The extinction coefficient $\kappa 1$ is calculated as $\kappa 1 = -10 \times \ln (i_0)$, i.e., $\kappa 1$ is valid for the very uppermost layer by fitting the values of i_0 of Grenfell and Maykut (1977) observed for the 0.1 m level in the ice. For example, $\kappa 1 = 17\ m^{-1}$ for clear sky (C=0) and white ice conditions. Below 0.1 m in the ice, we used $q_i(z,t) = i_0\cdot(1-\alpha_i)Q_s\ e^{-\kappa 2(z-zi)}$, z ≥ zi, according to Maykut and Untersteiner (1971), where $\kappa 2 = 1.5\ m^{-1}$. A two-layer scheme for $q_i(z,t)$ has been

used earlier by Sahlberg (1988) with a linear profile fitting the i_0 of Grenfell and Maykut(1977) at 0.1m in the ice. In snow, the variation of solar radiation absorbed with depth in snow follows simply the Bouguer-Lambert Law, i.e., $q_s(z,t) = (1-\alpha_s)Q_s\,e^{-\kappa sz}$, where the extinction coefficient of snow (κs) varies from 5 m^{-1} for dense snow up to almost 50 m^{-1} for newly-fallen snow, depending on the snow density and grain size (Perovich, 1996).

One can realise that estimation of $\partial q(z,t)/\partial z$ using a finite difference approach would yield different results using different spatial resolutions.

SIMULATIONS AND RESULTS

Model runs compared with analytical solutions

Analytical solutions for idealized cases were derived and compared with the numerical results. Three simplified model cases which can yield analytical solutions are defined: 1) Stefan ice growth model; 2) a parabolic diffusion equation with prescribed boundary condition of Dirichlet and Neumann type; 3) steady state of 2).

In case 1), the ice model yields a quite good consistency with the Stefan's ice growth in terms of various spatial resolution. This procedure can be used for verification of the numerical scheme. Increasing the model time step (coarser temporal resolution), the model runs with high spatial resolution showed an oscillation of the ice growth rate. Such numerical perturbations can be attenuated by adopting the numerical scheme into a fully implicit form. Case 2) showed that the modelled ice temperature approaches the analytical solution by increasing spatial resolution for both Dirichlet and Neumann boundaries (Fig. 1) and the accuracy improving exponentially. Case 3 illustrated the asymptotic state where the solar radiation tends to drive the temperature profile. In such a condition, a high resolution is needed for the numerical model in order to approach well the analytical solution, especially for the Neumann boundary (Fig 2).

Numerical experiments

The full heat conduction equation can not be solved analytically. Therefore groups of simulations were made, applying average climatic weather forcing data. The forcing data are taken from the Baltic Sea ice climate database IDA (Haapala et al. 1996). Three winters representing a normal (1983/84), a severe (1986/87) and a mild (1991/92) ice season were selected as typical Baltic winter climate scenarios. The meteorological data (air temperature T_a, wind speed V_a, relative humidity Rh, and cloudiness C) observed at Kemi, a meteorological station in the northern Baltic Sea (latitude 65.6° N) were used with fixed values. Each parameter is simply averaged over the three winters and for each month. The model runs are accordingly made for December, March and April corresponding to the ice-freezing, ice-thermal equilibrium and ice warm-up seasons. The solar radiation is incorporated as a monthly average diurnal cycle.

For the ice growth season, the initial ice thickness is taken to be 0.05m without snowfall. For the ice equilibrium stage, the initial snow and ice thicknesses are 0.3 m and 0.6 m respectively, in accordance with the monthly average from IDA. The spatial resolution of the ice layer is defined as $\Delta h_i = H_{i0}/N_i$, where H_{i0} is the initial ice thickness and N_i is the number of grid points. In the simulations we let N_i take every integer from 3 to 10, and then even integers from 12 to 32, i.e., a total of 19 spatial resolutions is used. The spatial resolution of the snow layer is defined as $\Delta h_s = H_{s0}/N_s$, where H_{s0} is the initial snow thickness; we let N_s vary from 3 to 15, while the snow thickness is assumed to remain constant. For the warm-up season, only bare ice with an initial thickness $Hi_0 = 0.7$ m is considered. The time step (τ) we used here is from 600s up to 6 hours.

The effect of the numerical resolution on model results can be summarized as follows:

(1) During the freezing season, the model yields quite accurate results compared with analytical solutions, indicating that the classical linear ice temperature model is still valid with reasonable accuracy. Figure 3 shows that the sensitivity of the results to numerical resolution occurs for large values of the ratio of the time step (s) to the grid size (m). This sensitivity can be decreased by using a fully implicit scheme or by reducing the value of this ratio. Resolution tends more to affect model results for short-term predictions. After adjustment to the initial conditions, the ice growth rate converges with decreasing grid size and resolution has no significant influence on model predictions. A large time step should be avoided under conditions of a rapid ice growth.

37

(2) During the ice thermal equilibrium stage, a low spatial resolution model yields a large diurnal variation in the surface temperature. The magnitude of solar radiation absorbed in the surface layer tended to complement the surface conductive heat flux (Fig. 4). The daily average surface temperature and net surface heat flux were less sensitive to the model spatial resolution. The impact of the spatial resolution on the model results is the greatest near the surface because of the strong gradient in the absorbed solar radiation.

(3) For the warm up season, the daily minimum surface temperature is sensitive to the spatial resolution. The strongly attenuated solar radiation absorbed in the surface layer was found to modulate the effect of grid resolution on the melting. The sub-surface maximum ice temperature can be simulated only with a high spatial resolution model (Fig. 5). Model run with a low spatial resolution may damp out the effect of penetrating solar radiation on the ice temperature profile. In late spring when the air temperature is well above the freezing point, the ice is warmed from the surface in response to the high air temperature, and the effect of penetrating solar radiation for model runs using various spatial resolutions tends to be minor.

For most thermodynamic ice models (e.g., Maykut and Untersteiner, 1971, Gabison, 1987, Ebert and Curry, 1993), the contribution of the absorbed solar radiation is divided explicitly by assuming a certain portion (0.17-0.35) of the total amount used in (1) and the rest used for the surface heat balance (2). This corresponds to a relatively weak effect of penetrating solar radiation $q(z,t)$ inside the ice. On the other hand, however, the grid spacing in these models was greater than 0.1m, satisfying the physical distribution of $q(z,t)$, i.e., a strong exponential decay near the surface. However, with a grid spacing less than 0.1m, the contribution of absorbed solar radiation should be adapted from the partition assumed above. This is particularly important for process studies of sub-surface melting of ice or snow. For example, Boggild et al. (1995) modelled the sub-surface melting by implementing an ice model using a resolution of 0.03m near the surface. The results of Fig. 5 implicitly indicate that sub-surface melting cannot be modelled with a coarse spatial resolution model.

Finally, we should emphasize that our studies correspond to somewhat simplified constant external forcing conditions so that the results on the effect of resolution depend on the validity of such an assumption. Other simplifications are made in connection with the optical properties of snow or ice, such as considering separately the surface albedo and the extinction coefficient. The results presented were obtained using an Eulerian grid, but additional sensitivity studies indicated that similar characteristics can be obtained using a Lagrangian grid. We suggest that for process studies, an ice model should apply a time step of about 600s and a spatial resolution of 2 – 5 cm in ice or snow, if possible. For climatological studies, an relaxation of resolution is certainly needed, but the ratio of time step to grid size should remain small.
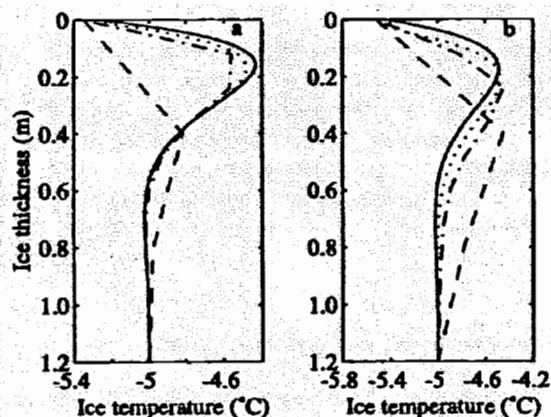
Figure 1.   The vertical ice temperature profile obtained by an analytic solution (solid line) and the numerical model using spatial resolutions of N_i = 3 (broken line), 10 (dot-dashed line) and 30 (dotted line). The boundary conditions are of the Dirichlet (a) and Neumann (b) type. Each ice temperature profile corresponds to a time near mid-day.
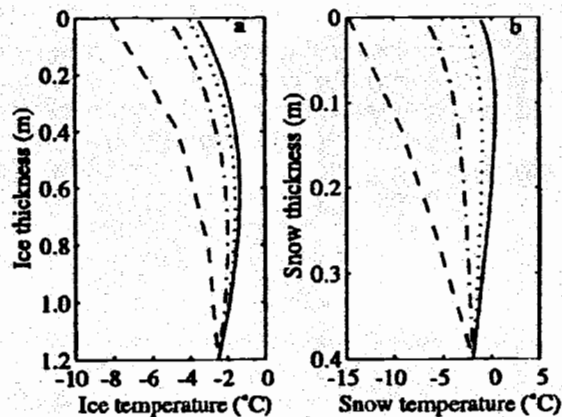
Figure 2.   Vertical temperature profile in ice (a) and snow (b), obtained by the analytic solution (solid line) and the a numerical model using as its spatial resolution $N_{i,s}$ = 3 (broken line), 10 (dot-dashed line) and 30 (dotted line). The boundary condition is of the Neumann type.

38
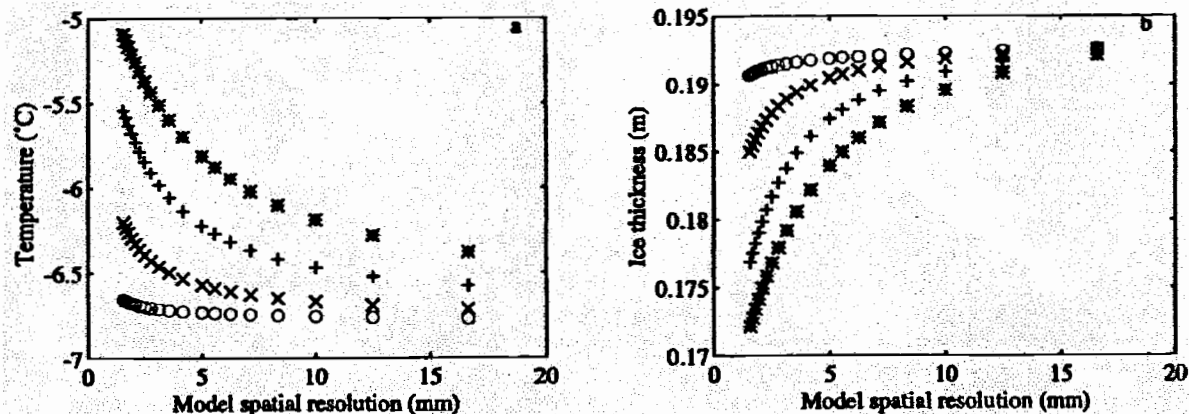
Figure 3. Modelled average surface temperature (a) and total ice formation (b) during the ice growth season for a 5-day period versus spatial resolution. Each symbol indicates a given time step, i.e. 600s (o); 1 hour (x); 3 hours(+); and 6 hours (*).
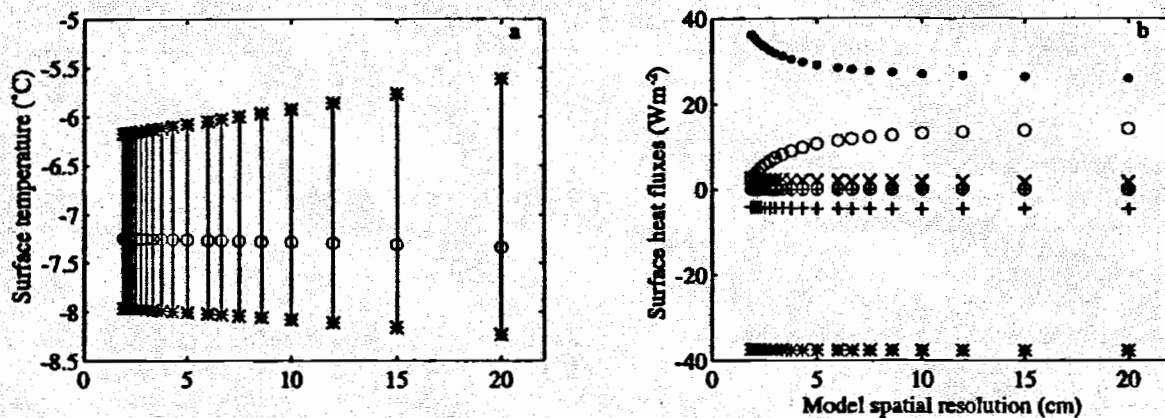
Figure 4. (a) Modelled daily variation of surface temperature in March (on the 5th day modelled) versus spatial resolution. The stars indicate the daily maximum (upper) and minimum (lower) surface temperatures, while the circles give the average daily surface temperature. (b) Modelled daily average surface heat fluxes versus model spatial resolution. Each symbol refers to a term in the surface heat flux: net long-wave radiation flux (*), sensible heat flux (x), latent heat flux (+), absorbed solar radiation in the surface layer (o), conductive heat flux (•), and net surface heat flux (⊕). Calculations are made for bare ice.

39
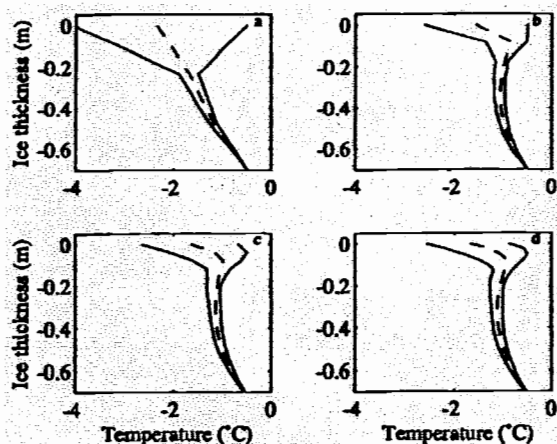
Figure 5. Modelled in-ice temperature profile using spatial resolutions of (a) 23 cm, (b) 8.75 cm, (c) 3cm and (d) 2.5 cm. The corresponding values of N_i are: 3, 8, 18, and 28, respectively. In each panel, the three lines indicate respectively the daily minimum (left), daily average (middle) and daily maximum (right) in-ice temperature.

Table 1. Model parameters based on field measurements in the Baltic Sea and values found in the literature.

|	
Density of air (ρ_a)	1.26 kgm^{-3}
Specific heat of air (c_p)	1004 J kg^{-1} K^{-1}
Extinction coefficient of sea ice (κ_i)	1.5 – 17 m^{-1}
Extinction coefficient of snow (κ_s)	15 – 25 m^{-1}
Freezing point (T_f)	–0.3 °C
Heat capacity of ice (c_0)	2093 J kg^{-1} K^{-1}
Latent heat of freezing (L_f)	0.33×10^6 J kg^{-1}
Oceanic heat flux (F_w)	1.0 W m^{-2}
Density of ice (ρ_0)	910 kg m^{-3}
Salinity of sea ice (s_i)	1.5 ppt
Salinity of water below sea ice (s_w)	5 ppt
Density of snow (ρ_s)	310 kg m^{-3}
Surface albedo of sea ice	0.7
Surface albedo of snow	0.8
Thermal conductivity of ice (k_{i0})	2.03 W m^{-1} K^{-1}
Thermal conductivity of snow (k_s)	0.24 W m^{-1} K^{-1}
Solar constant (S)	1367 W m^{-2}
Boltzmann constant (σ)	5.68x10^{-8} Wm^{-2} K
Constant (β)	0.117 W m^{-1} ppt^{-1}
Constant (γ)	17.2 ×10^6 J Km^{-3} ppt^{-1}
Time step of model (t)	600 s – 6 hours
Number of layers in the ice	3 – 32

REFERENCES

Andreas, E. L. 1987. A theory for the scalar roughness and the scalar transfer coefficients over snow and sea ice. Boundary-Layer Meteorol., 38, 159--184.

Bennett, T.J. 1982. A coupled atmosphere-sea-ice model study of the role of sea-ice in climatic predictability. J. Atmos. Sci. 39, 1456–1465.

Boggild, C.E., J.G. Winther, K. Sand and H.Elvehoy. 1995. Sub-surface melting in blue-ice fields in Dronning Maud Land, Antarctica: Observation and modelling. Ann. Glaciol., 21. 162 – 68.

Cheng B. 1996. The conservative difference scheme and numerical simulation of a one-dimensional thermodynamic sea ice model, M. Sci. Bull., 15(4), 8--15 (in Chinese).

Ebert, E.E. and J.A. Curry. 1993. An intermediate one-dimensional thermodynamic sea ice model for investigating ice-atmosphere interaction. J. Geophys. Res., 98(C6), 10,085–10,109.

Efimova, N.A. 1961. On methods of calculating monthly values of net long-wave radiation. Meteorol. Gidrol., 10, 28–33.

Gabison R. 1987. A thermodynamic model of the formation, growth, and decay of first-year sea ice. J. Glaciol., 33(113), 105–109.

Grenfell, T.C. and G.A. Maykut. 1977. The optical properties of ice and snow in the Arctic Basin. J. Glaciol., 18(80), 445–463.

Haapala, J. et al. 1996. Ice data bank for Baltic Sea climate studies. Report Series in Geophysics, 35. Dept. of Geophysics, University of Helsinki.

Holtslag, A. A. M and H. A. R. de Bruin. 1988. Applied modelling of the nighttime surface energy balance over land. J. Appl. Meteorol., 37, 689–704.

Högström, U. 1988. Non-dimensional wind and temperature profiles in the atmospheric surface layer: a re-evaluation. Boundary-Layer Meteorol., 42, 55–78.

Jacobs, J.D. 1978. Radiation climate of Broughton Island. In: Barry, R.G. and Jacobs, J.D. (eds): Energy budget studies in relation to fast-ice breakup processes in the Davis Strait. Occas. Pap. 26: 105-120. INst. of Arctic and Alp. Res., Univ. of Colo., Boulder.

Launiainen, J and B. Cheng. 1998. Modelling of ice thermodynamics in natural water bodies. Cold Reg. Sci. Technol., 27(3), 153-178.

Li, R.H and G.C. Feng. 1980. Numerical solutions of differential equation. Publishers of High Educations,China (in Chinese).

Liston, G.E., J.G. Winther, O. Bruland, H. Elvehoy and K. Sand. 1999. Below-surface ice melt on the coastal Antarctic ice sheet. J. Glaciol., 45(150), 273–285.

Maykut, G.A and N. Untersteiner. 1971. Some results from a time dependent thermodynamic model of sea ice. J. Geophys. Res., 76(6), 1550–1575.

Maykut, G.A. 1978. Energy exchange over young sea ice in the central Arctic. J. Geophys. Res., 83(C7), 3646–2658.

Perovich, D.K. 1996. The optical properties of sea ice. Cold Regions Research and Engineering Laboratory (CRREL) Report 96-1, Hanover, NH.

Sahlberg, J. 1988. Modelling the thermal regime of a lake during the winter season. Cold Reg. Sci. Technol., 15(2), 151–159.

Semtner, A.J., 1976. A model for the thermodynamic growth of sea-ice in numerical investigation of climate. J. Phys. Ocean., 6, 379-389.

Shine, K.P. 1984. Parameterization of short-wave flux over high albedo surfaces as a function of cloud thickness and surface albedo. Q. J. R. Meteorol. Soc., 110, 747–764.

Shirasawa, K., K. Kobinata and T. Kawamura. 2001. Eddy Flux measurements below ice and ocean boundary layer studies. In Launiainen, J. and T. Vihma (eds.): BALTEX-BASIS Final Report 2001, Geesthacht, Germany. International BALTEX Secretariat. (Publication 19). 170–178.

Untersteiner, N. 1961. On the mass and heat budget of Antarctic sea ice. Arch. Meteorol. Geophys. Bioklim., Series A, 12: 151–82.

Untersteiner, N. 1964. Calculations of temperature regime and heat budget of sea ice in the central Arctic. J. Geophys. Res., 69(22), 4755–4766.

On the Sensitivity of Baltic Sea Ice Variability to Changing Climate

MARKUS MEIER

One of the goals of the Swedish Regional Climate Modeling Program (SWECLIM) is to simulate long-term changes and natural variability of the Baltic Sea. AN essential feature of the Baltic is the seasonal ice cover. Normally, the ice season lasts 5–7 months, from November to May. Interannual variability of the ice extent is large. During a mild winter, ice occurs only in the northernmost sub-basin, the Bothnian Bay, while in a cold winter the whole Baltic Sea can become ice-covered. As surface albedo changes drastically with ice conditions, sea ice in the Baltic is regarded as a key element in the North-European climate system. In addition, Baltic Sea ice extent and mean winter temperature in North and Central Europe are strongly correlated. The ice extent is fairly well correlated to the North Atlantic Oscillation (NAO) index during winter. However, the relationship is not stationary over time.

In this study, Baltic Sea ice variability in changing climate is investigated using a 3D coupled ice–ocean model, the Rossby Centre Ocean model (RCO). RCO is a further development of the Ocean Circulation Climate Advanced Modeling Project model (OCCAM). As the OCCAM project focuses on global scales it was necessary to add parameterizations important for the Baltic Sea. A two-equation turbulence closure scheme, open boundary conditions, and a sea ice model were main features that had to be added for our purposes.

The ocean model in RCO is coupled with a Hibler-type two-level (open water and ice) dynamic-thermodynamic sea ice model. An extension of the widely used viscous-plastic rheology with an elastic component leads to a fully explicit numerical scheme that improves computational efficiency, particularly on high resolution grids, and adapts easily to parallel computer architectures. The ice thermodynamics are based on Semtner's layer models for thick ice/snow (multiple layers) and thin ice/snow ('zero'-layer) using characteristic discrimination thicknesses for ice and snow. In RCO thick ice consists of one or two ice layers and thick snow consists of one snow layer. Snow is converted to snow ice if flooding as calculated

from Archimedes' Law occurs. The equations of the ice model are discretized on the same Arakawa B-grid used for the ocean with a horizontal resolution of 6 nautical miles.

As a reference, long hindcast simulations have been performed. For the period 1902-1998, atmospheric surface data have been reconstructed. Whereas 100-year long records of river runoff and sea level data are available, an observational data set of atmospheric surface fields applicable to force a 3D coupled ice-ocean model of the Baltic Sea is lacking. Therefore, a statistical model has been developed to reconstruct daily sea level pressure and monthly surface and dew-point temperature, precipitation, and cloud cover fields on a one degree times one degree regular horizontal grid. The statistical model works reasonably well for all variables. The results of the ice model are compared with observations from monitoring stations, ice charts and satellite data. The observed seasonal and interannual variability of sea ice is well reproduced by the model.

To investigate sea ice variability in changing climate, two sets of 30-year time slice experiments have been performed using a fully coupled regional atmosphere-ice-ocean model (RCAO), one representing pre-industrial greenhouse conditions (control simulation), and the other a global warming based upon the A2 emission scenario from the IPCC Special Report on Emission Scenarios (SRES). The lateral boundary conditions of the regional model are taken from the global HadCM3 model from the Hadley Centre. The scenario simulation is a projection of future climate for the period 2070-2100, whereas the control simulation refers to the period 1960-1990. In the control run, the mean seasonal cycle of ice cover and its variability is simulated realistically compared to observations, but the seasonal ice cover maximum is somewhat lower than observed and the simulated mean melting date comes somewhat earlier. The decrease of mean ice extend in the scenario, compared to the control run, of 64 percent is dramatic. However, in all scenario years, ice is still formed in the Bothnian Bay. The mean number of ice days decreases also significantly.

Model dependent uncertainties with impact on simulated ice variability and its change are discussed and the downscaling results are compared with earlier studies performed at the Rossby Centre and at the University of Helsinki with a different ice model.

Towards Accurate Sea-Ice Modeling in a Coupled MM5/Sea-Ice Model: Treatment of the Ocean

JING ZHANG[1], JEFFREY S. TILLEY[1] AND XIANGDONG ZHANG[2]
[1]Geophysical Institute, University of Alaska, Fairbanks, AK 99775
[2]International Arctic Research Center, University of Alaska, Fairbanks, AK, 99775

Recent evidence of sea-ice concentration and thickness decreases as well as warming of oceanic upper- and mid-levels has been hypothesized to be caused by amplified global warming within the higher latitudes of the Northern Hemisphere. As such, the proper specification of sea-ice and ocean properties has become a topic of considerable importance in model evaluation and climate change assessment.

A coupled MM5/Sea-ice model has been developed and applied to the Pan-Arctic region in which a thermodynamic sea ice model is included to replace the simple treatment of sea ice in the standard MM5 model. In the standard MM5 model, sea ice concentration is treated as a binary function (either 100% or 0 over a grid cell). Our coupled system allows sea-ice concentration to range from 0–100% and to be a prognostic quantity. A comparison of the simulations with the standard MM5 and the coupled system over the Pan-Arctic region shows substantial sensitivity in the resulting atmospheric simulation (e.g., surface air temperature, sensible and latent heat fluxes, boundary-layer structure) to the sea ice treatment at daily and bi-weekly time scales.

However, coupled simulations are not without their limitations. In particular, ocean temperature is prescribed with sea surface temperature (SST); it can either be held constant at the initial values or vary on a daily timescale as prescribed from NCAR/NCEP reanalysis data. This approach, while common for regional operational or research models where the simulation length is less than 5 days, has some

fundamental problems for the Arctic. First, it is not possible to get an adequate ocean temperature representation under the sea-ice cover or in leads with routinely available observations. Second, since neither SST nor mixed layer temperatures (the critical value at the ice bottom surface) are predicted quantities, substantial errors in the ocean/ice heat flux exchanges can result, particularly if there are errors in the ocean temperature initial state. In addition, during the transition season, the ocean surface layer may have strong mixing and a diurnal cycle which cannot be represented. To correct these problems it is necessary to better represent ocean mixed layer processes.

In this study, an ocean mixed layer model (MLM) is coupled to the coupled MM5/Sea-ice system to improve treatment of ice/ocean interactions and simulations of sea-ice concentration/thickness, SST variation and flux exchanges between the atmosphere, ice and ocean. We will present the simulation results from the new coupled system MM5/Sea-ice/MLM and address the influence of the ocean on the sea-ice and atmosphere.

Modelling of Sea Ice Thermodynamics and Air–Ice Coupling During Warm-Air Advection

BIN CHENG AND TIMO VIHMA

Finnish Institute of Marine Research, P.O. Box 33, FIN-00931 Helsinki, Finland

The modelling sea ice thermodynamics is usually considered as a one-dimensional process. This is a good approximation with respect to the heat conduction within the snow and ice as well as the mass balance. In conditions of a large horizontal temperature gradient in the overlying atmosphere, the effects of this gradient is, however, reflected in the sea ice thermodynamics as well. During advection of warm air over an initially cold sea ice surface, there is an interaction between the cooling of the air mass and heating of the upper layers of the ice and/or snow. The magnitude and spatial scale of these cooling and heating processes depend on the meteorological situation: on the temperature of the air, snow, and ice, on the cloud cover, solar radiation, surface albedo, wind speed, and air humidity as well as on the fetch over the ice. A two-dimensional mesoscale atmosphere model is coupled with a sea ice model to simulate the sea ice thermodynamics and air-ice coupling. Spatial attention is paid to the different meteorological conditions with respect to the radiative forcing: cases of clear and overcast skies during the polar night and spring time are studied. These cases are simulated with a wide range of atmospheric pressure gradients, i.e. the geostrophic wind driving the ABL flow varied from 2 to 24 m s^{-1} in various simulations. In addition, we study the effect of the snow cover. The structure of the model is shown in Figure 1.
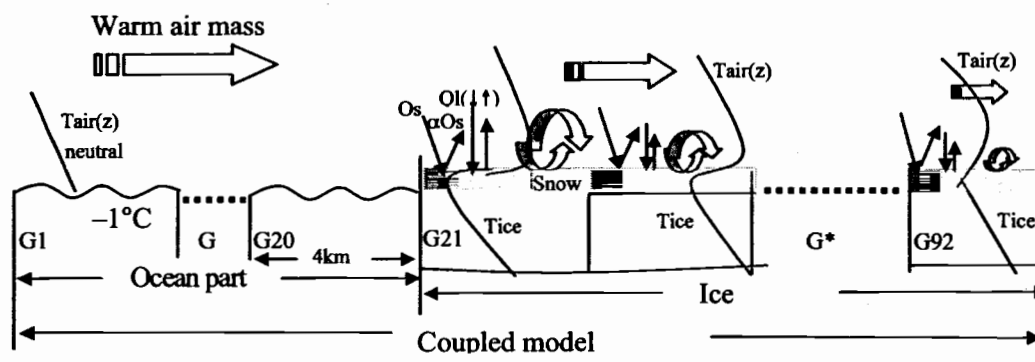

Figure 1. Structure of the coupled ABL–sea ice model. The first 20 grid cells from the inflow boundary represent open sea with a fixed surface temperature and a fixed inflow temperature profile ($\partial T/\partial z = -6.5$ K km^{-1}). The rest of the grid cells (72) represent sea ice with or without a snow cover.

A total 96 model runs were made under different external conditions. The ice temperature demonstrated a vertical and horizontal redistribution in response to the local surface heat balance, and a large horizontal temperature gradient developed in the atmosphere due to the cooling of the air mass. The ice temperature regime revealed intensive modification near the ice edge due to a strong air-ice turbulent heat exchange. The air mass became simultaneously colder downwind of the ice edge, and therefore less ice temperature modification was found far from the ice edge. The diurnal variation of temperature in the upper ice/snow layer is related to that of the downward solar radiation. On the other hand, increasing wind speed enhances the turbulent heat exchange between air and ice, and thus the diurnal variation of the ice temperature decreases. In cloudy conditions the downward longwave radiation and turbulent heat flux tend to dominate the surface heat balance. An almost isothermal layer often develops in the upper ice layer in the upwind part of the ice-covered region. In addition, with a strong wind the entire upper ice/snow layer may become warmer in balance with a consistent initial upward heat flux in deeper ice/snow. Under overcast skies during spring, the horizontal surface ice/snow mass balance in response to warm air advection revealed a wind speed dependence. In conditions of a strong wind a large portion of surface melting may be associated with the strong turbulent heat exchange. From the point of view of ABL modelling, the interactive coupling between the air and ice was most important when the wind was strong, while from the point of view of ice thermodynamic modelling the coupling was most important when the wind was light.

THEME 4: Sea-ice and Ocean Observations

Small-Scale Kinematics from RADARSAT SAR Imagery

RON KWOK

High-resolution radar imagery of the Arctic Ocean is being acquired on a routine basis. These sequential radar observations, collected by RADARSAT, are transformed into estimates of ice motion, deformation, age and thickness by the RADARSAT Geophysical Processor System (RGPS).The RGPS data products provide basin-scale views of the evolution of the sea ice cover over an entire winter based on continued sampling of Lagrangian elements on the ice cover. At any given time, the data products allow the visualization of all the kinematically active linear features over the Arctic Ocean. Nearly all deformations on the ice cover are localized along these features while the rest of the ice cover remains unaffected. These long, narrow fracture features may contain open water, new ice, nilas, young ice, first-year ice, rafted ice, or ridged ice. They can be created by divergence, convergence, or shear. The amount of open water production, ridging and the thin ice thickness distribution can be estimated at these linear features. Here, we show the temporal development of the characteristics of these features from thee years of RGPS measurements of the Arctic Ocean ice cover.

Small Scale Fast Ice Processes: Implications for the Coastal Regime and Large Scale Models

ANDREW MAHONEY, HAJO EICKEN AND LEW SHAPIRO

A fundamental component of the Arctic coastal zone, fast ice extends from the shoreline to the inshore boundary of the shear zone where it interacts with the drifting pack ice. The dynamic processes of this environment are complex and have significant differences from those in the drifting pack ice. Though they are often too small to be resolved in large scale dynamic models, the impacts of these processes can be far-reaching, affecting nearshore and shelf circulation as well as ice–ocean interaction.

As a component of the ocean, fast ice acts as a hindrance to navigation and as a conduit to transmit stress over large distances, making it an essential consideration for shipping and nearshore development in the Arctic. Acting as an extension of the land, it serves to protect the coast from erosive forces of ocean and ice. In addition the ice is used as a habitat by Arctic wildlife and for subsistence hunting activities by native peoples.

Ice-ocean interaction within the nearshore zone is strongly affected by the fast ice, which diminishes momentum transfer between the atmosphere and ocean and represents an important constraint for the nearshore tidal components. Beneath the fast ice, therefore, there can exist a large volume of water isolated from the atmosphere and experiencing little thermohaline driving due to reduced bottom freezing rates. Thus at the fast ice edge, which is the site of significant new-ice formation, there can be complex thermohaline circulation.

Given the concentration of population, industry and infrastructure at the coast in the Arctic, improved modeling of the nearshore zone would be of benefit for many future activities. More research is required to allow sea ice-ocean models of higher spatial resolution to adequately represent the processes governing the cycle of fast ice establishment and decay. In the meantime, however, observations of fast-ice distribution and evolution may help in improving model performance in the coastal zone and over the narrow parts of the Beaufort and Chukchi shelves.

Though a primitive fast ice climatology can be derived from observations, the state of the fast ice is governed by a number of covarying dynamic and thermodynamic processes leading to a complex evolution through the ice year and great interannual and spatial variability. For the fast ice to be incorporated as a

component of large scale sea ice models, these processes need to be understood and implemented at an appropriate scale.

Here we present some fundamental processes responsible for the formation, deformation and break-up of fast sea ice in the Alaskan Arctic together with their linkages to large scale forcing, such as sea surface temperature, nearshore sea ice thickness and concentration, surface wind speed and direction, nearshore bathymetry, coastal currents.

Peculiarities of the Vertical Temperature and Salinity Water Structure in the Melt Ponds on the Land Fast and Drifting Ice

IVANOV, B.V.[1], MAKSHTAS A.P.[1,2], ANDREEV O.M.[1], BOGORODSKY P.V.[1]
[1]Arctic and Antarctic Research Institute, St. Petersburg, Russia
[2]International Arctic Research Center, University of Alaska, Fairbanks, USA

The results of direct field measurements of the vertical distributions of water temperature (T) and salinity (S) in the melt ponds are analyzed for the land fast ice (Barrow, 2001) and drifting ice (the Laptev and Barents Seas, 1993, 1996). It is shown that in the deep melt pond with a crack on the bottom or melt pond adjusted to a ridge, the water temperature and salinity distributions had well expressed two-layer structure similar to the observation in the Arctic Seas. The experiment with artificial mixing of the pond water had shown that the complete recovery of such structure occurred after 24 hours. The preliminary estimates show that the coefficient of vertical mixing in the investigated salt melt pond closes to the estimated one in the freshwater melt ponds in the Laptev Sea ($10^{-6} \times 10^{-6}$ m²/s).

The role of radiation and convective processes in the melt pond formation is considered. It is shown that heat fluxes caused by the absorption of short-wave radiation in a water column of a melt pond and in the underlying ice cover (melt pond bottom) are approximately the same, mainly in overcast. The simple one-dimensional numerical model reproducing peculiarities of the temporal variability of the vertical T-S structure in a melt pond (formation of warm interior layers, salinity shocks, etc.) is described.

The efficiency of convection in the freshwater melt pond, originated due to upper surface heating or short-wave radiation absorption, in the bottom melting is studied within the framework of the modified Rayleigh-Benard problem for two layer binary fluid.

The Importance of the Interactions Between Landfast Ice and Pack Ice for Models of the Nearshore Chukchi and Beaufort Seas

LEWIS SHAPIRO, HAJO EICKEN AND ANDREW MAHONEY
Geophysical Institute, University of Alaska Fairbanks

For the foreseeable future, it is likely that most impact in the Arctic related to exploration and production of resources and expanded surface transportation will take place within about 200 km or less from the nearest coastline. That area includes (1) the landfast ice zone, (2) the shear zone where deformation between the landfast ice and the pack ice takes place, (3) part of the pack ice zone, and, (4) the area occupied by "stable extensions" of the landfast ice which may extend that zone seaward for various time periods.

The purpose of this paper is to describe some properties of the ice, and patterns and modes of deformation that are characteristic of those areas, and to explain their significance to developing models of processes in the nearshore Chukchi and Beaufort Seas.

The area being considered here is generally ice-free at the end of summer. Even when ice is present in any of the zones defined above at that time of year, it consists of loose floes not joined into a continuous ice cover. New ice is introduced into the area during "freeze up", which can be a period of significant ice motion. In protected areas, the ice simply freezes in place, but elsewhere much of the "new" ice consists of floes of first-year or multiyear ice that are driven into the nearshore area by wind and ocean currents. These movements result in the formation of shear and pressure ridges, grounded hummock fields and other deformational features within and on the boundary of the landfast ice. The process of extending the landfast ice seaward by relatively large jumps (as opposed to the addition of single, isolated ridges) along the Beaufort Sea coast has been observed to extend through the winter and well into March. As the landfast ice area grows seaward, the configuration of its offshore edge changes in a manner that, on a large scale, tends to smooth out its boundary with the shear zone. This is important for model development, because the shape of the boundary influences the patterns and intensities of the stress fields that are transmitted deeper into the pack ice during interactions across the shear zone. Similar considerations apply as the ice deteriorates during breakup and into the summer. Thus, the interaction between the ice in these zones provides an important boundary condition on models of pack ice deformation for the nearshore area, but one that changes through the year.

There are repeatable patterns of deformation that are characteristic of the nearshore areas of both the Chukchi and Beaufort Sea coasts at various times of year that reflect the processes noted above. The descriptions and illustrations of these will be presented.

Reevaluation of Water Mass Tracers in Arctic Ocean

NORI TANAKA
Frontier Research System for Global Change, IARC

In the summer of 1999 and 2000, extensive integrated observations have been carried out by using R/V *Mirai*, which is operated by JAMSTEC. Hydro-casts and seawater sampling have carried out for physical and biogeochemical studies during the cruises around Bering shelf, Chukchi and Beaufort Seas.

In 1999, there was distinctive intrusion of warm water around 20–40 m depth was found in further north of Chukchi Sea. The water is believed to be Pacific in origin based on stable isotope systematics and N** values. In 2000, the intrusion of the water mass in subsurface layer was less pronounced.

Stable isotope of seawater is being used for differentiating water masses in Arctic Ocean. Over 1200 seawater samples were analyzed for stable oxygen isotope ratio for this study. Salinity–$\delta^{18}O$ relationship revealed distinctive Atlantic, Pacific seawater end-member points, and also mixing with fresh water (river and ice melt) and brine formed during sea ice formation. Startlingly, water mass with the $\delta^{18}O$ and salinity values accepted for typical Pacific water in Arctic Ocean could not be found. It could jeopardy the feasibility of the estimation of pacific water fraction in the previous studies.

Barium (one of alkali-earth elements) has been used for American river input in Arctic without checking its conservativeness for tracing water masses. In order to evaluate biological alternation of barium, its contents in surface layer water after river water mixing with high barium concentration (600 nmol/kg for McKenzie water) is obtained based on fiver water fraction of seawater estimated by $\delta^{18}O$ systematics. By comparing with actually observed concentration, as great as 50% of barium reveals to be removed from seawater, presumably by biological uptake. Because of the substantial alteration, barium should be used as a water mass tracer after appropriate correction for biological effects or under oceanographic conditions in which biological processes for barium is not active such as under thick multi-year ice zone.

Experience of Supporting Users with Specialized Information on Ice Cover State

IGOR APPEL

INTRODUCTION

Increasingly we see the industrialization of arctic and sub-arctic areas with mining, oil exploration, and fishing. As a consequence of these developments, the improvement of scientific-operational systems to support ice navigation in arctic and sub-arctic seas has significant economic and social importance.

An increase of activities in ice-infested waters will require not only more detailed and accurate, but also specialized ice information meeting various requirements of different users.

Ice information tailored to the individual requirements of a user could be characterized as specialized information, as opposed to more generalized information on ice cover state supplied by numerical models.

GENERAL APPROACH TO SUPPORT

- The modern system of ice support includes the following constituent elements:
- observations on ice cover and influencing factors;
- numerical methods of ice simulation and forecasting;
- specialized information and recommendations for decision-making.

Mean values of simulated geophysical ice state parameters for a numerical grid cell often cannot be used to meet customer requirements. Proposed design of scientific-operational system supporting customers with information on ice state includes ice model and statistical blocks translating output of numerical calculations into specialized information or recommendations for practical applications. These two components of the system are combined together on the basis of using results of additional theoretical or empirical researches. The components successfully supplement each other and give necessary reliable information about all ice parameters required by a customer.

There are two main aspects of using ice information critically important to practical applications. First of all, it should be taken into account that ice cover even at the scale of fine model resolution is essentially inhomogeneous. The second feature of using ice information for practical applications is connected with the need to estimate objectively the influence of ice cover state upon different kind of industry activities.

OBSERVATIONS ON ICE STATE

On the whole, ice cover is a very complicated media consisting of numerous constituent elements. The term "ice state" implies a wide set of parameters characterizing properties of actual ice cover. A description of ice state can be done for the local area, for the entire sea or any of its parts. In principal, ice conditions can be called ice state or ice regime for any scale.

We believe that it is not reasonable to try to develop a comprehensive definition of ice state, because ice cover causes different influence on different activities in ice-infested waters. Therefore, support of those activities with ice information must meet different requirements and deal with various properties and features of ice cover.

For many tasks, the complete set of required information on ice cover state could not be obtained without field observations on mesoscale inhomogeneity of ice parameters, forms of floating ice, ridge configuration, and physical properties of ice.

Field observations play an important role in the development of models and as ground truth. Therefore close interrelation between environmental observers and authors of numerical methods is a necessary condition to increase the accuracy and quality of ice support.

It is necessary to emphasize that numerous interesting datasets were collected by industry and could be very useful for development and testing numerical ice models. Among such data are hourly observations from oil rigs on ice drift and parameters of ice cover state. Another example includes frequent maps of ice distribution accompanied by photos of ice conditions collected during air reconnaissance in support of testing contingency plans for events of an oil spill in ice covered waters.

NUMERICAL MODELING OF ICE STATE

A dynamic thermodynamic ice model developed by the author is used to simulate and forecast ice cover state. The wide use of the model demonstrated its applicability to decide different theoretical and applied problems. One older variant of the model has being used for many years in operational activity of the Ice Information Center at the Arctic and Antarctic Research Institute, St. Petersburg, Russia.

Theoretical description of internal interaction in ice cover is based on the following physical assumptions. First of all, ice cover responses differently to compression and tension. Tensile stresses could not exist in ice cover. Secondly, in the most cases, compressive and tensile strains are presented in ice cover simultaneously. Normal stresses are significantly anisotropic.

Thirdly, ice cover response differently to shear and compression. Within the frameworks of continuum description of ice cover it is valid to use principal axes of stress and strain tensors to distinguish shear and compression.

Shearing plays the key role in failure of ice floes. Namely shearing causes appearance of linear discontinuities. Initially it is a slip line (or crack) that can be transformed either in shear ridge or lead depending on other influencing conditions.

Developed mathematical model of anisotropic ice cover describes diversity of ice stress states, was successfully applied to quite different ice conditions in coastal areas and in the central part of the Arctic Ocean. The model simulates typical orientation of leads forming in ice cover in the vicinity of a coast line, islands, and arched leads at approaches to straits.

The model takes into account the influence of thermal factors on the state of ice cover that are important even for short-term calculations. In the summer period, inhomogeneity of ice thickness is usually attributed to irregular melting, explained mostly by upper ice surface morphology and redistribution of melt water.

The mathematical model describes ice cover as a geophysical phenomenon with resolution on the order of 10 km. At the same time, the model takes into account some important subgrid features of ice behavior and distribution.

In particular, the model describes influence of a narrow boundary layer of significant shear deformations near a coastal line (barrier islands).Allowing for this layer gives a more precise description of spatial changes in ice velocity near a coastal line. It significantly increases accuracy of simulating ice deformation and corresponding processes of ridging in the vicinity of a coast.

Another subgrid description is applied to the simulation of ice edge location. Knowledge on exact configuration of ice edge is meaningful for various practical offshore works. The information on ice edge location is used in the model to improve mathematical description of dynamic and thermodynamic processes.

Original algorithm of calculating advective changes in ice parameters is based on allowing for local changes in parameters within grid cells. The approach suppresses undesirable influence of computational viscosity.

RESULTS

Results of using discussed model underwent detailed considerations. Numerical methods created of the basis of the model have successfully found wide application in calculations of current and future ice conditions. To support users, a three-to-four-day forecast is considered as a primary planning tool and an one-to-two-day forecast allows us to take into account more detailed information about extreme events such as hazardous pressure in ice cover.

The model allows reliable simulation of redistribution of ice cover for the entire summer period without accumulation of significant errors and development of long-term ice forecasts for several months in advance. We would like to emphasize that the quality of ice simulations does not depend upon sign or magnitude of ice anomaly in every specific year. It has been shown that the method has a high quality of modeling interannual changes in ice concentration for seas with different ice regime.

A similar method is also used for short-term (several days) ice forecasts of ice edge position, thickness, concentration (including partial), and the location of compaction areas. Observations on oil rigs

demonstrate that the method successfully simulates local changes in concentration characterized by large short-term variability.

Reliability of calculating intensity and orientation of compacting has been confirmed by observation data from ships. We need to note that shipboard observations on ice compacting are the only source of reliable data as even data of visual air reconnaissance are essentially different.

EXAMPLE OF SPECIALIZED SUPPORT
1. Planning navigations
All parameters of ice cover state are characterized by significant mesoscale variability. The collected onboard simultaneous observations on ice cover parameters and ship or icebreaker velocity in ice-infested waters are used to study ice inhomogeneity and create an empirical model of vessels motion. Field experiments give necessary data for comparative analysis of ice distribution along the actual meandering ship path and average values of ice parameters in the region of operations.

2. Ice loads
Determination of ice loads on offshore engineering structures needs information on numerous parameters of ice cover state. Ice models give valuable information on forces and deformations in ice cover. But those data differ significantly from real loads on structures.

Two additional steps are required to transform parameters averaged for grid cells into local conditions. The first involves transition from a continuum medium to composite discrete elements. The second corresponds to transition from deterministic parameterization to a stochastic description. Field observations on ice cover are used to get probabilistic distribution of the parameters describing local ice conditions for the area of observations.

CONCLUSIONS
The detailed analysis of scientific operational ice support for offshore exploration in Arctic made almost 10 years ago led to the following conclusion. Close cooperation and feedback between government agencies, scientific community, and explorations companies as well as the creation of special task force would be necessary to decide problems of supporting offshore activities.

Observations and Modeling of Small-Scale Thermodynamic Ice Growth and Decay Processes in Coastal Arctic Seas

H. EICKEN[1], D. K. PEROVICH[2], T. C. GRENFELL[3], K. FREY[1], L. H. SHAPIRO[1], A. MAHONEY[1]
[1]Geophysical Institute, University of Alaska Fairbanks, Fairbanks, AK, USA
[2]Cold Regions Research and Engineering Laboratory, Hanover, NH, USA
[3]Department of Atmospheric Science, University of Washington, Seattle, WA, USA

In discussing the present status and future directions of ice-ocean modelling and in particular the adequate representation of smaller-scale processes and phenomena, the issue of predicting the thermodynamic (i.e., static) growth and melt of sea ice is typically considered a problem not as pressing as those related to ice dynamics. This is well justified by the excellent performance of even simpler ice-growth models (such as 0+ layer model by Semtner [1976] and recent improvements such as those of Bitz and Lipscomb [1999]) in predicting the thickening of level ice. The inverse square-root dependence of growth rate on thickness dependence furthermore helps to dampen errors in initial or boundary conditions when predicting ice growth. Nevertheless, as will be shown in exemplary ice-mass balance data obtained near Barrow, Alaska, the key role of the snow cover in controlling heat transfer through the ice slab still represents a formidable challenge insofar as the snow cover is highly variable both in space and time.

However, the key challenge facing the entire suite of ice-growth/decay models remains the prediction of summer ablation and complete ice decay. In this presentation, by drawing on data collected at the Surface Heat Budget of the Arctic Ocean (SHEBA) ice camp and in first-year fast ice off Barrow in 1998 to 2001, we

will address the two core components of this problem, one generic to all Arctic ice-covered regions, the second specific to the nearshore zone.

First, it needs to be considered that currently even the most sophisticated models parameterize the surface albedo of melting sea ice, dominated mostly by the areal fraction and state of melt ponds. In turn, most of these parameterizations prescribe the albedo by (implicitly or explicitly) prescribing the seasonal progression of the pond fraction. Field observations suggest that fully predicting surface albedo may be inherently very difficult, though alternative approaches can help mitigate this problem. At the same time, however, current parameterizations of first-year and coastal ice albedo as employed in large-scale GCMs are largely inadequate and can introduce substantial errors. We propose to address this problem through field observations.

The second problem is mostly unique to nearshore and fast ice, but has considerable consequences in particular with respect to coastal dynamics and infrastructure. Thus, ablation rates of nearshore ice are significantly enhanced in some areas by advective heat fluxes due to riverine discharge (Searcy et al. [1996], Bareiss et al. [1999]). Here, prediction of ice melt and decay requires a full consideration of the local hydrology, which can vary substantially from year to year. Furthermore, observations of high surface ablation rates at Barrow suggest that advective turbulent heat transfer in the atmosphere can also play an important role and may need to be considered. Finally, nearshore sea-ice is often characterized by low to high concentrations of sediment inclusions that have a significant impact on the heat budget of the ice cover (Frey et al. [2001]).

The presentation will conclude with an assessment of the tractable and intractable aspects of these problems and attempt to outline directions for future improvements.

On the Excitation of Natural Shelf Modes Due to Self-Induced Oscillations of Ice Floes by Ridges Buildup

A. MARCHENKO[1], A. MAKSHTAS[2] AND L. SHAPIRO[3]
[1]Theoretical Department, General Physics Institute of RAS, Vavilova str. 38, 119991 Moscow, Russia
[2]International Arctic Research Center, University of Alaska Fairbanks, Fairbanks, AK 99775-7340
[3]Geophysical Institute, University of Alaska Fairbanks, Fairbanks, AK 99775-7335

Field observations under the landfast sea ice near Point Barrow Alaska, recorded vertical displacements of several centimeters amplitude and of an order of 600's period (Bates and Shapiro, 1980). Assuming that typical period of irregular displacements of ice floes due to pressure ridge buildup between them has an order of ten minutes (Marchenko and Makshtas, 2001), we speculate that gravity waves of such period could be excited by the transfer of ice floes impulse in the water.

In the accordance with this hypothesis the dynamic problem on the compression of circular floes under the influence of onshore wind is considered. It is shown that the compression realized by irregular displacements of the floes in onshore direction even exist in the cases when wind velocity is a constant. Therefore these oscillations can be called as self-induced oscillations. Two types of self-induced oscillations are found. Oscillations with periods of several tens of minutes are excited due to the interaction between the ridging and continuous ice, which is accumulated at the seaward boundary of continuous ice. Oscillations with periods of several minutes and less are excited due to the interaction of a few ridge build up events between the floes.

Then we analyze the frequencies of natural modes of water oscillations on shelf region near Point Barrow. It is shown that second shelf mode, whose length in normal direction to the coastline is two times smaller than the shelf width, has period of the order 600 s. Thus, self-induced oscillations of the floes producing impulse transfer in the water can be the source of effective excitation of the natural shelf modes.

Bates, H.F., and L.H. Shapiro, 1980. Long-period gravity waves in ice-covered sea. J. Geophys. Res., Vol. 85, NC2, 1095-1100.

Marchenko, A., and A. Makshtas, 2001. Ice ridging over various space scales. J.P. Dempsey and H.H. Shen (ed.), IUTAM Symposium on Scaling Laws in Ice mechanics and Ice Dynamics, 103-114, Kluwer Academic Publishers.

KAZUTAKA TATEYAMA
Hokkaido University

In winter, the Sea of Okhotsk is generally almost entirely covered with sea ice from late November to late May. Even in the southernmost part of the sea, along the northeastern sea coast of Hokkaido, the sea in general starts to freeze at early January and is covered with sea ice till late March. In the coastal regions off Hokkaido unstable ice pack found were, some consisting of drift ice from the north and others of locally frozen fast ice, and also found were packs of double or triple rafted ice.

The Sea Ice Research Laboratory(SIRL) of the Institute of Low Temperature Science, Hokkaido University was founded in Mombetsu in February 1966 to conduct studies mainly on sea ice and coastal oceanography. The SIRL has successively operated a sea-ice monitoring radar network on the Okhotsk coast of Hokkaido since 1969. The network consists of three landbased radars which allow a continuous monitoring of realtime ice field scenery along a 250-km coastline to as far as about 50 km into the Okhotsk Sea.

Variability and Climate Sensitivity of the Fast Ice Extent in the Northeastern Part of the Kara Sea

DMITRY DIVINE[1], REINERT KORSNES[2], ALEXANDER MAKSHTAS[3]
[1]Norwegian Polar Institute, Tromso, Norway; email: dmitry.divine@npolar.no
[2]Norwegian Defence Research Establishment, Kjellern,Norway; email: reinert.korsnes@ffi.no
[3]International Arctic Research Center, Fairbanks, Alaska, USA; email: makshtas@iarc.uaf.edu

The temporal and spatial variation of shore-fast ice extent in the northeastern part of the Kara Sea during 1953–1999 is investigated and its sensitivity to interannual variability of regional climate is estimated. Regular observations by the Arctic and Antarctic Research Institute (AARI) during 1953–1990 and SSM/I surface brightness temperatures during 1987–2000 provide data on the fast ice extent. Monthly means air temperature, snow depth and precipitation rate recorded by meteorological polar stations located in the study area are used to assess an influence of atmospheric conditions on the fast ice extent. Wind velocity and direction measured on the Dikson Island are used to estimate an influence of the wind stress on the fast ice extent. Monthly means of the Ob and Enissey discharge in 1950–1987 are used as well.

Data analysis shows a significant correlation (about –50%) between mean winter temperature anomalies and the average fast ice area in May for all meteorological stations located in the study area. No significant correlations were found between fast ice extent and cumulative winter precipitation as well as with average snow depth during winter. This differs from results reported for the Canadian Arctic fast ice. Analysis of the sensitivity of fast ice extent to the wind direction shows significant role that the strong eastward and south-eastward winds play in fast ice formation during a winter season. This is indicated by correlation of the same order (–50%) as for average winter temperature anomalies. Wind data analysis also indicates that winds from northeast during June–July increase fast ice destruction while winds from northwest tends to restrain it. No correlations were found between the fast ice extent and the preceding summer river outflow rate.

The area of fast ice in spring months shows clear bimodal distribution. This indicates the existence of two different regimes of fast ice formation driven by prevailing winds. Time series records of shore fast ice area show a steady decrease in 1953–1990. The decrease is most pronounced in May. The shore fast ice in the northeastern part of Kara Sea seems to break up early in the period 1980–1990 compared to 1953–1960.

52

SIOM Workshop Participants

Igor APPEL
Science Systems & Applications Inc.
320 N Street SW
Washington, D.C. 20024
Phone: (301) 286-9088
Fax: (301) 286-8624
E-mail: iappel@earthlink.net

Andrew BRYDON
Department of Mathematics & Statistics
University of New Mexico
Albuquerque, New Mexico 87131
Phone: (505) 730-0704
Fax: (505) 424-4254
E-mail: brydon@unm.edu
Website: www.math.unm.edu

Bin CHENG
Finnish Institute of Marine Research
P.O. Box 33
FIN-00931, Helsinki, Finland
Phone: 358-9-61394427
Fax: 358-9-3231025
E-mail: bin@fimr.fi
Website: www2.fimr.fi

Max COON
Northwest Research Associates, Inc.
P.O. Box 3027
Bellevue, Washington 98009-3027
Phone: (425) 644-9660
Fax: (425) 644-8422
E-mail: max@nwra.com
Website: www.nwra.com

Hajo EICKEN
Geology/Geophysics Department
Geophysical Institute
University of Alaska, Fairbanks
P.O. Box 757320 / 903 Koyukuk Dr.
Fairbanks, Alaska 99775-7320
Phone: (907) 474-7280
Fax: (907) 474-7290
E-mail: hajo.eicken@gi.alaska.edu
Website: www.gi.alaska.edu/~eicken

Daniel FELTHAM
Centre for Polar Observation and Modelling
CPOM, Department of Space and Climate Physics
University College
Gower Street
London, United Kingdom WCIE 6BT
Phone: +44 (0) 20 7679 3017
Fax: +44 (0) 20 7679 7883
E-mail: daniel.feltham@cpom.ucl.ac.uk
Website: www.cpom.org

Roland W. (Bill) GARWOOD, Jr.
Department of Oceanography
Naval Postgraduate School
833 Dyer Road, Room 328
Monterey, California 93943-5193
Phone: (831) 656-2673
Fax: (831) 656-2712
E-mail: garwood@nps.navy.mil
Website: www.oc.nps.navy.mil/opbl

Jari HAAPALA
Department of Physical Sciences
University of Helsinki
P.O. Box 64
Helsinki, Finland FIN-00014
Phone: +358-9-1915 1015
Fax: +358-9-1915 1000
E-mail: Jari.J.Haapala@helsinki.fi
Website: www.physics.helsinki.fi

Kate HEDSTROM
Arctic Region Super Computing
University Of Alaska Fairbanks
910 Yukon Drive
Fairbanks, Alaska 99775
Phone: (907) 474-7896
Fax: (906) 474-5494
E-mail: kate@arsc.edu
Website: www.arsc.edu

William D. (Bill) HIBLER III
International Arctic Research Center
Frontier Group
P.O. Box 757335 / 930 Koyukuk Dr.
Fairbanks, Alaska 99775-7335
Phone: (907) 474-7254
Fax: (907) 474-2643
E-mail: billh@iarc.uaf.edu
Website: www.frontier.iarc.uaf.edu

Mark A. HOPKINS
U.S. Army Corps of Engineers ERDC-CRREL
72 Lyme Road
Etna, New Hampshire 03755
Phone: (603) 646-4249
Fax: (603) 646-4477
E-Mail: mark.a.hopkins@erdc.usace.army.mil

Motoyoshi IKEDA
Graduate School of Environmental Earth Science
Hokkaido University
North 10, West 5
Kita-ku, Sapporo, Japan 060-0810
Phone: 81-11-706-2360
Fax: 81-11-706-4865
E-mail: mikeda@ees.hokudai.ac.jp

Meibing JIN
International Arctic Research Center
Frontier Group
P.O. Box 757335 / 930 Koyukuk Dr.
Fairbanks, Alaska 99775-7335
Phone: (907) 474-6877
Fax: (907) 474-2643
E-mail: mbj@ims.uaf.edu
Website: www.frontier.iarc.uaf.edu

Ron KWOK
Jet Propulsion Laboratory
300-235 4800 Oak Grove Drive
Pasadena, California 91109
Phone: (818) 354-5614
Fax: (818) 393-3077
E-mail: ron.kwok@jpl.nasa.gov
Website: www-radar.jpl.nasa.gov/rgps

Qinzheng LIU
National Marine Environment Forecast Center
8, Dahuisi Road, Haidian District
Beijing, 100081, China
Phone: (8610) 62173322 Ext. 146 or 150
Fax: (8610) 62173620
E-mail: qzliu@axp800.nmefc.gov.cn

Aleksey MARCHENKO
General Physics Institute
Russian Academy of Sciences
Kantemirovskays Street, 18/2-363
115409 Moscow, Russia
Phone: 7-095-320-8710
Fax: 7-095-135-0270
E-mail: amarch@orc.ru or amarch@kapella.gpi.ru

Jennifer HUTCHINGS
International Arctic Research Center
Frontier Group
University of Alaska, Fairbanks
P.O. Box 757335 / 930 Koyukuk Dr.
Fairbanks, Alaska 99775-7335
Phone: (907) 474-7569
Fax: (907) 474-2643
Website: www.iarc.uaf.edu

Boris IVANOV
Arctic & Antarctic Research Institute
38 Bering Street
St. Petersburg, Russia 199397
Phone: (812) 3523352/(812) 3520069
Fax: (812) 3522685/(812) 3522688
E-mail: b_ivanov@aari.nw.ru
Website: www.aari.nw.ru

Walter JOHNSON
Minerals Management Service
381 Elden Street
Herndon, Virginia 20170-4817
Phone: (703) 787-1642
Fax: (703) 787-1053
Website: www.mms.gov/eppd/sciences/osmp/index.htm

Ron LAI
Minerals Management Service
381 Elden Street
Herndon, Virginia 20170-4817
Phone: (703) 787-1714
Fax: (703) 787-1053
E-mail: ronald.lai@mms.gov
Website: www.mms.gov/eppd/sciences/osmp/index.htm

Andrew MAHONEY
Geophysical Institute
University of Alaska, Fairbanks
P.O. Box 757320 / 903 Koyukuk Dr.
Fairbanks, Alaska 99775-7320
Phone: (907) 474-5648
Fax: (907) 474-7290
E-mail: mahoney@gi.alaska.edu
Website: www.gi.alaska.edu/~mahoney

Wieslaw MASLOWSKI
Oceanography Department
Naval Postgraduate School
Monterey, California 93943
Phone: (831) 656-3162
Fax: (831) 656-2712
E-mail: maslowsk@oc.nps.navy.mil
Website: www.oc.nps.navy.mil/~pips3

54

H.E. Markus MEIER
Swedish Meteorological & Hydrological Institute
Rossby Centre
SE -- 601 76
Norkoping, Sweden
Phone: ++46 (0) 11-495 8612
E-mail: markus.meier@smhi.se
Website: www.smhi.se/sgn0106/rossby/start.htm

Leif Toudal PEDERSEN
Technical University of Denmark
Oersted*DTU, Building 348
Lyngby, Denmark DK-2800
Phone: +45 45253791
Fax: +45 45931634
E-mail: ltp@oersted.dtu.dk
Website: www.dcrs.dtu.dk/DCRS/seaice/latest-ice.html

Robert S. PRITCHARD
IceCasting, Inc.
20 Wilson Court
San Rafael, CA 94901-1230
Phone: (415) 460-1565 (home)
Phone/Fax: (415) 454-9899 (work)
E-mail: pritchardr@asme.org
Website: www.icecasting.com

Chuck SAMUELS
Fairweather, Inc.
715 L Street
Anchorage, Alaska 99501
Phone: (907) 258-3446
Fax: (907) 279-5740
E-mail: chuck@fairweather.com

Howard L. (Buck) SCHREYER
Department of Mechanical Engineering
University of New Mexico
Albuquerque, New Mexico 87131
Phone: (505) 299-3102
Fax: (505) 277-1571
E-mail: schreyer@me.unm.edu

Caryn SMITH
Minerals Management Service
949 East 36th Avenue
Anchorage, Alaska 99508-4363
Phone: (907) 345-4082
Fax: (907) 345-6805
E-mail: caryn.smith@mms.gov
Website: www.mms.gov

Motoyasu MIYATA
Yokohama Institute for Earth Sciences
3173-25, Showa-machi, Kanazawa-ku
Yokohama, Kanagawa, 236-0001, Japan
Phone: +81-45-778-5615
Fax: +81-45-778-5497
E-mail: miyata@jamstec.go.jp

Richard PRENTKI
Environmental Assessment of Offshore Oil Development
Minerals Management Services Alaska OCS Region
949 East 36th Avenue, 3rd Floor
Anchorage, Alaska 99508-4363
Phone: (907) 271-6599
Fax: (907) 271-6111
E-mail: richard.prentki@mms.gov
Website: www.mms.gov/Alaska

Francois ROY
Institute Maurice-Lamontagne
Fisheries and Oceans Canada
850, Route de la Mer
Mont-Joli, Canada G5H 3Z4
Phone: (418) 775-0641
Fax: (418) 775-0546
E-mail: royf@dfo-mpo.gc.ca

François SAUCIER
Institute Maurice-Lamontagne
Fisheries and Oceans Canada
850, Route de la Mer
Mont-Joli, Quebec, Canada G5H 3Z4
Phone: (418)775-0791
Fax: (418)755-0542
Email: saucierf@dfo-mpo.gc.ca
Website: www.qc.dfo-mpo.gc.ca/iml/en/scientists/saucierfj
Website: www.qc.dfo-mpo.gc.ca/iml/fr/chercheurs/saucierfj

Lewis SHAPIRO
Geophysical Institute
University of Alaska, Fairbanks
P.O. Box 757320 / 903 Koyukuk Dr.
Fairbanks, Alaska 99775-7320
Phone: (907) 474-7196
Fax: (907) 474-7290
E-mail: lews@gi.alaska.edu
Website: www.gi.alaska.edu

Deborah SULSKY
Department of Mathematics&Statistics
University of New Mexico
472 Humanities Building
Albuquerque, New Mexico 87131
Phone: (505) 277-7425
Fax: (505) 277-5505
E-mail: sulsky@math.unm.edu
Website: www.math.unm.edu/~sulsky

Kazutaka TATEYAMA
Hokkaido University
6-4-10 Minamigaoka
Hokkaido, Japan 094-0013
Phone: +81-1582-33722
Fax: +81-1582-35319
E-mail: tateyama@pop.lowtem.hokudai.ac
Website: www.lowtem.hokudai.ac.jp/english/index.html

Noriyuki TANAKA
International Arctic Research Center
University of Alaska Fairbanks
P.O. Box 757335 / 930 Koyukuk Drive
Fairbanks, AK 99775-7335
Phone: (907) 474-2687
Fax: (907) 474-2643
E-mail: norit@iarc.uaf.edu
Website: www.frontier.iarc.uaf.edu

Ryan WALKER
Courant Institute of Mathematical Sciences
New York University
251 Mercer St., MC-0711
New York, New York 10012
Phone: (212) 998-3207
Fax: (212) 995-4121
E-mail: walkerr@cims.nyu.edu

Keguang WANG
University of Helsinki, Division of Geophysics
Gustaf Hallsrominkata 2
P.O. Box 64
Helsinki, Finland FIN-00014
Phone: 358-9-19151002
Fax: 358-9-19151000
E-mail: keguang.wang@helsinki.fi
Website: http://geophysics.helsinki.fi

Xiangdong ZHANG
International Arctic Research Center
Frontier Group
University of Alaska Fairbanks
P.O. Box 757335 / 930 Koyukuk Dr.
Fairbanks, Alaska 99775-7335
Phone: (907) 474-2675
Fax: (907) 474-2643
E-mail: xdz@iarc.uaf.edu

Jeffrey TILLEY
Atmospheric Science Group
Geophysical Institute
University of Alaska, Fairbanks
P.O. Box 757320 / 903 Koyukuk Dr.
Fairbanks, Alaska 99775-7320
Phone: (907) 474-5852
Fax: (907) 474-7290
E-mail: jeff@gi.alaska.edu
Website: www.gi.alaska.edu/AtmosSci/tilley/webpage.html

Petteri UOTILA
Courant Institute of Mathematical Sciences
New York University
251 Mercer St., MC-0711
New York, New York 10012
Phone: (212) 998-3245
Fax: (212) 995-4121
E-mail: uotila@cims.nyu.edu
Website: http://gamma.nic.fi/~hpuotila/cv.html

Jia WANG
International Arctic Research Center
Frontier Group
P.O. Box 757335 / 930 Koyukuk Dr.
Fairbanks, Alaska 99775-7335
Phone: (907) 474-2685
Fax: (907) 474-2643
E-mail: jwang@iarc.uaf.edu
Website: www.frontier.iarc.uaf.edu

Jing ZHANG
Geophysical Institute
903 North Koyukuk Drive
P.O. Box 757320
University of Alaska Fairbanks
Fairbanks, Alaska 99775-7320
Phone: (907) 474-1539
Fax: (907) 474-7290
E-mail: jin@rathlin.iarc.uaf.edu
Website: www.gi.alaska.edu

Denis ZYRYANOV
Norwegian Polar Institute
The Polar Environmental Centre
N-9296 Tromso, Norway
Phone: +47 77 75 05 43 or +47 77 75 05 00
Fax: +47 77 75 05 01
E-mail: denis.zyryanov@npolar.no
Website: www.npolar.no

The Department of the Interior Mission

As the Nation's principal conservation agency, the Department of the Interior has responsibility for most of our nationally owned public lands and natural resources. This includes fostering sound use of our land and water resources; protecting our fish, wildlife, and biological diversity; preserving the environmental and cultural values of our national parks and historical places; and providing for the enjoyment of life through outdoor recreation. The Department assesses our energy and mineral resources and works to ensure that their development is in the best interests of all our people by encouraging stewardship and citizen participation in their care. The Department also has a major responsibility for American Indian reservation communities and for people who live in island territories under U.S. administration.

The Minerals Management Service Mission

As a bureau of the Department of the Interior, the Minerals Management Service's (MMS) primary responsibilities are to manage the mineral resources located on the Nation's Outer Continental Shelf (OCS), collect revenue from the Federal OCS and onshore Federal and Indian lands, and distribute those revenues.

Moreover, in working to meet its responsibilities, the **Offshore Minerals Management Program** administers the OCS competitive leasing program and oversees the safe and environmentally sound exploration and production of our Nation's offshore natural gas, oil and other mineral resources. The MMS **Royalty Management Program** meets its responsibilities by ensuring the efficient, timely and accurate collection and disbursement of revenue from mineral leasing and production due to Indian tribes and allottees, States and the U.S. Treasury.

The MMS strives to fulfill its responsibilities through the general guiding principals of: (1) being responsive to the public's concerns and interests by maintaining a dialogue with all potentially affected parties and (2) carrying out its programs with an emphasis on working to enhance the quality of life for all Americans by lending MMS assistance and expertise to economic development and environmental protection.